RIJKSWATERSTAAT COMMUNICATIONS

No. 25

MOTORWAY TUNNELS BUILT BY THE IMMERSED TUBE METHOD

by

IR. A. GLERUM

IR. B. P. RIGTER

IR. W. D. EYSINK

W. F. HEINS

1976

RIJKSWATERSTAAT COMMUNICATIONS

MOTORWAY TUNNELS BUILT BY THE IMMERSED TUBE METHOD

by

IR. A. GLERUM
Locks and Weirs Department, Rijkswaterstaat

IR. B. P. RIGTER
Locks and Weirs Department, Rijkswaterstaat

IR. W. D. EYSINK
Delft Hydraulics Laboratory

W. F. HEINS
Soil Mechanics Laboratory, Delft

Government Publishing Office - The Hague 1976

All correspondence should be addressed to

RIJKSWATERSTAAT

DIRECTIE WATERHUISHOUDING EN WATERBEWEGING

THE HAGUE – THE NETHERLANDS

The views in this article are the authors' own.

ISBN 90 12 01188 4

Contents

1 Introduction

The concept of a tunnel is very general. A classification can be made by use, geographical conditions, type of construction and so on.
Tunnel engineering is not only very extensive, it is also ancient: a tunnel with a length of 1 km is thought to have been built under the Euphrates more than 4,000 years ago to link the royal palace with a temple. The course of the river was temporarily diverted during the construction. In our modern world the idea of building a tunnel for a purpose like that in ancient Babylon is no longer conceivable, but the technique of temporarily diverting a waterway in whole or in part is still used. Examples are provided in the Netherlands by the Velsen tunnel [lit. 2] the aqueduct under the Haarlemmermeer Ringvaart and the Gouwe tunnel.
This paper is concerned primarily with a different type of tunnel which may be defined as follows on the basis of the classification criteria mentioned above.
Use: road traffic with the emphasis on motorway tunnels.
Geographical conditions: sub-aqueous crossings.
Method of construction: immersed tube method with subsequent cut and cover construction on the banks.

The first sub-aqueous crossing in the shape of a tunnel in the Netherlands was the Maas tunnel at Rotterdam, opened to traffic in 1942 [lit. 1]. Although construction by the immersed tube method was not new (the first application of this method dates back to 1893), the type of construction differed from that developed in the United States: the cross-section was not circular but rectangular, and steel, which was the principal structural material in American tunnels, played only a secondary role as a water seal. The actual structure was in reinforced concrete.
Subsequently, reinforced concrete immersed tube tunnels were further developed in the Netherlands. Table 1 lists the road tunnels built in this way. The same method has also been used for the subway tunnel in Rotterdam [lit. 8] and for two pipeline tunnels, one of which is about 1,700 m long [lit. 9].
The general geometry of motorway tunnels in the Netherlands is decribed in chapter 2; in section 2.1.3 special attention is given to the relationship between the required traffic clearances and the resulting cross-section of an immersed tube tunnel.
Some aspects of the design and construction of immersed tube tunnels and the adjoining sections on the waterway banks are discussed in chapter 3. A new development is described in section 3.2, i.e. the omission of the watertight lining resulting for the first time in a genuine 100% reinforced concrete structure.
Sections 3.3 and 3.4 contain contributions by the Delft Hydraulics Laboratory and

the Soil Mechanics Laboratory, Delft, respectively; these establishments normally advise the agency which designs motorway tunnels, the Locks and Weirs Department of the Rijkswaterstaat. The other chapters were contributed by the latter organization and for the traffic aspects discussed in sections 2.1.1 and 2.2.1 use was made of directives, data, etc. supplied by the Traffic Engineering Department of the Rijkswaterstaat.

Table 1 *Summary of Netherlands road tunnels (existing and under construction)*

Name	Date of opening or planned completion	Number of traffic lanes[1]	Length of closed section (m)	Overall length[2] (m)	Method of construction	Client	Reference in Literature
Maas[3]	1942	2×2[4]	1070	1373	Immersed tube	Rotterdam	1
Velsen	1957	2×2	768	1644	Cut & cover	Rijkswaterstaat	2
Coen	1966	2×2	587	1283	Immersed tube	Rijkswaterstaat	3
Schiphol	1966	$2\times3+2\times2$[5]	530	660	Cut & cover	Rijkswaterstaat	
Benelux	1967	2×2	795	1300	Immersed tube	Benelux tunnel N.V.[8]	4
Heinenoord	1969	$2\times(2+1)$[6]	614	1064	Immersed tube	Rijkswaterstaat	5
IJ[3]	1969	2×2	1037	1685	Immersed tube	Amsterdam	6
Vlake	1975	2×3	327	773	Immersed tube	Rijkswaterstaat	7
Drecht	1977	4×2	555	825	Immersed tube	Rijkswaterstaat	24
Kil	1977	$2\times(2+1)$[6]	406	901	Immersed tube	Stichting Tunnel Dordtse Kil[8]	25
Prinses Margriet	1977	2×2[7]	77	938	Immersed tube	Rijkswaterstaat	26

[1] The first figure indicates the number of traffic tubes and the second the number of lanes per tube.
[2] Length of closed section + open access sections.
[3] Urban motorway tunnels (N.B. *the others are rural motorway tunnels*)
[4] Plus one tube for pedestrians and one for cyclists.
[5] Each of the 2×3 tubes also includes an emergency stopping lane; the tubes with 2 lanes are intended for local traffic.
[6] $2+1$ = 2 lanes forming part of the motorway + 1 lane for slow traffic.
[7] Each tube also includes an emergency stopping lane.
[8] Designed by the Locks and Weirs Department of the Rijkswaterstaat.

2 Dimensions of road tunnels

2.1 Cross-section

2.1.1 *Traffic and maintenance requirements*

A tunnel generally forms a short section of a highway. This means that the principal criteria applicable to the route as a whole should also be followed in the design of the tunnel. Basic factors such as the number of lanes, their width and the vertical clearance in the tunnel should be the same as on the rest of the road. More specifically, for motorway tunnels, this means a lane width of 3.50 m and a vertical clearance of 4.50 m. The lanes are separated from each other by broken paint lines with a width of 0.10 m, while the outer edges of the lanes are marked by continuous lines with a width of 0.15 m.
Outside the traffic lanes, however, the design of the tunnel crosssection differs considerably.
To begin with, the emergency stopping lanes which are normally treated as part of the cross-section of a motorway, will often be omitted in tunnels. In the Netherlands, the shallow Schiphol tunnel and the short Margriet tunnel are exceptions in this respect. In France too some tunnels have emergency stopping lanes, but once again these are exceptions from the normal type of tunnel.
The reason for omitting the emergency lane is a financial one. Although the cost of a tunnel does not rise in linear proportion to increasing width, the cost increase is not inconsiderable: if two 'narrow' emergency stopping lanes with a width of 2.50 m each are provided in a deep tunnel, the cost increase will be in the order of 10,000 guilders/m'. This is the cost of building an entire motorway including the necessary civil engineering works outside the tunnel. In some parts of the Netherlands a motorway can even be built for less than this.
The outright omission of emergency stopping lanes is not, however, possible on a motorway. Supplementary measures are necessary with a view to safety. Since the Coen tunnel, opened in 1966, it has become standard practice to provide tunnels which do not have emergency stopping lanes with traffic signals for each lane consisting of illuminated green arrows and red crosses suspended centrally above the lanes, both in the tunnel proper and on the approaches. Normally, the installation is out of service but as soon as a vehicle stops at any point, the lane concerned is 'closed' with the red crosses (this means that drivers must leave the lane as quickly as possible) and the green arrows indicate which lane (or lanes) are still open to traffic, albeit subject to a speed limit. The panels indicating this speed limit (generally 70 kph) are

set up before the entrance to the tunnel proper. Further up the road orange flashing lights are also switched on as a warning to approaching drivers.
This intervention is only possible if two requirements are met: detection of stationary or slow-moving vehicles and subsequent actuation of the signals. The problem is simplified by the fact that in most tunnels constant supervision is necessary to ensure that the ventilation, lighting and pump facilities are operational. The staff entrusted with this task are also made responsible for the traffic signals. As only one person is continuously present in the control room, the traffic is observed with the aid of television cameras mounted in the tunnel tubes and on the approaches. The information can be processed in two ways: the traffic may be observed continuously on several permanent monitor screens (Heinenoord tunnel) or else detector systems (radar, induction loops) can be used to switch onto two monitor screens the images from the two cameras scanning the section of the tunnel in which a deviant traffic situation has arisen (Coen and Benelux tunnels). The signals could conceivably be switched on directly by a computer but in practice this is not (yet) possible: detection of a speed which is too low gives an early warning. Whether the vehicle in fact comes to a standstill or leaves the tunnel slowly remains to be determined by television observation. The man in the control room must watch the situation carefully before he switches on the signalling system.
It is worth noting in passing that the telephones installed at intervals of 90 to 100 m in the right-hand wall to enable stranded drivers to call the control room are seldom if ever used. The control system in fact works more quickly.
The combination of these observation and signalling arrangements justifies the omission of emergency stopping lanes in motorway tunnels: even though a vehicle which is in difficulties cannot move away to the hard shoulder of the road, the risk of other vehicles running into it is limited by the fact that the lane concerned is immediately 'closed'.
Lateral clearances, i.e. the space between the traffic lane and tunnel wall are another point in which the tunnel differs from an open highway. The lateral clearances have two functions:
— to ensure the safety and smooth flow of traffic (level of service and capacity), the influence of the wall or other raised obstacles ('wall effect') must be limited as far as possible;
— safety of pedestrians must be guaranteed. The term 'pedestrians' includes both maintenance personnel and the occupants of vehicles who have to leave them in an emergency.

An ideal solution would be to arrange the facilities necessary for both functions next to each other: a level strip adjacent to the traffic lane and an elevated footway with an efficient safety barrier against the wall. This solution is, however, very expensive. In most tunnels therefore a compromise is struck between the two functions: a low footway (approximately 0.15 m) with a width of about 0.75 m.

The height is generally based on the following passage in the Highway Capacity Manual 1965 (page 89):

'*It is believed that mountable curbs or vertical curbs 6 inches or less in height have insignificant influence on traffic operations*'.

It should be noted here that the H.C.M. is concerned only with capacities and levels of service and does not consider traffic safety, although theoretically this factor should be discounted in the levels of the service.

This solution has been adopted in existing motorway tunnels in the Netherlands. An example is the Benelux tunnel (figures 1 and 2); this has a footway with a width of 1.20 m and a height of 0.30 m on the left and a 0.80 × 0.14 m footway on the right. On the outside edge, the higher footway has a special profile (TRIEF profile) intended to guide vehicles which collide with the footway. This elevated footway was specially intended for maintenance staff who can reach it through doors at intervals of 90 m from the central service gallery.

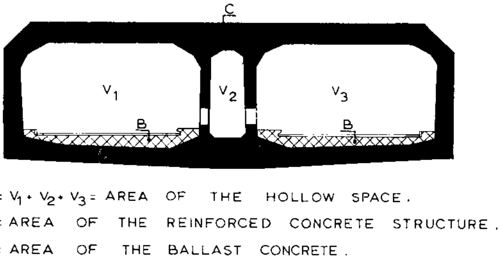

Figure 1. Cross-section of the Benelux tunnel.

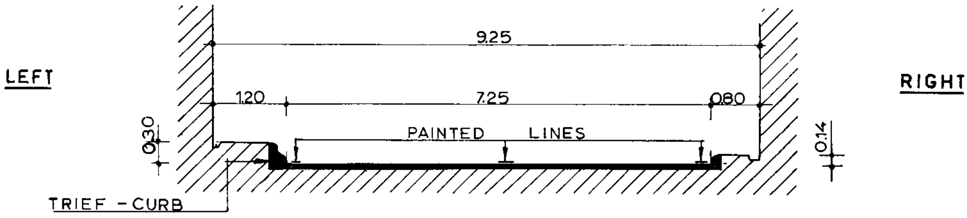

Figure 2. Cross-section of one of the traffic tubes of the Benelux tunnel.

Experience in the Netherlands has shown that footways only ensure relative protection to pedestrians.

Over a period of four years, three commercial vehicles and five cars have penetrated onto the 'elevated' footway on the left in the Benelux tunnel, while five commercial vehicles and one private car have done so during five years in the Coen tunnel. The fact that the low footways on the right-hand side offer only limited protection is shown by the many scrapes and scratches on the walls.

Prototype tests in the Netherlands have also shown that a low footway does not act as a barrier to traffic and therefore provides no real protection.

Because of these considerations, in existing Netherlands motorway tunnels, the traffic lane next to the footway is closed by the red crosses as soon as pedestrians are walking on the footway. The arrow and cross signals initially designed to avoid accidents caused by stationary vehicles have thus acquired a second function.
Because of this use of the signals, elevated footways have lost their role in providing (incomplete) protection to pedestrians. Experiments in the Netherlands have also shown that raised curbs or other obstacles (unless they are lower than 5 to 7 cm) next to the traffic lane present some danger to vehicles which have swerved off course (the vehicle may overturn or be deflected back in an unfavourable manner). The elevated footways with a TRIEF profile also gave poor results in this study:
If the angle of impact is greater than 2° the vehicle may overturn or be deflected back damaged; this will depend on the speed and height of the centre of gravity of the vehicle etc. Practical experience has shown similar results: over a period of four years, four incidents of this kind have been noted in the Benelux tunnel; in two cases the vehicle overturned and in the two others it was deflected back with damaged steering equipment.

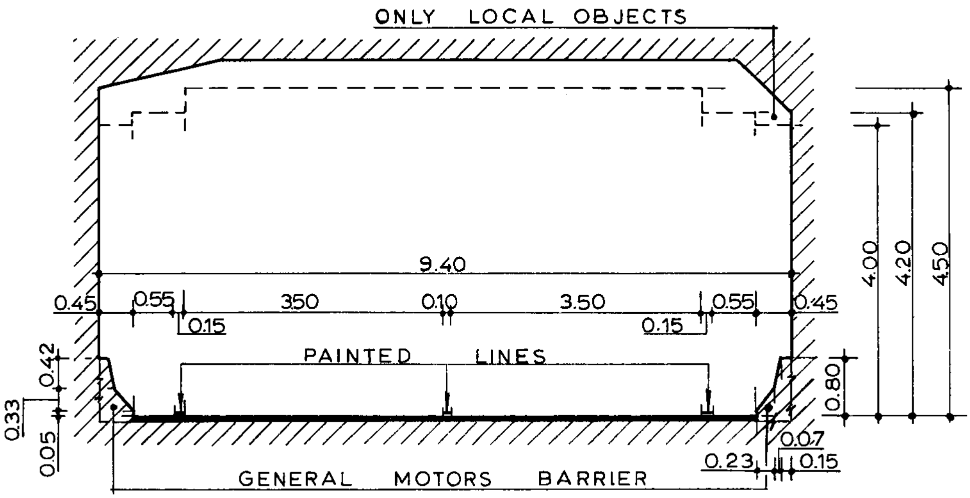

Figure 3. Cross-section of a 2-lane traffic tube of a new Dutch tunnel.

In the light of these observations and experience a different type of lateral clearances has been adopted for Netherlands motorway tunnels now under construction or projected; the arrangement is shown in figure 3 (see also lit. 10). Next to the traffic lane there is a level strip with a width of 0.55 m and against the wall a concrete curb with a width of 0.45 m. The curb has been developed by a leading American motor manufacturer and is known as the G.M. barrier after the company which designed it. Tests carried out in the United States have shown that private cars are not seriously damaged if the angle of impact is less than 10°; the corresponding figure for commercial vehicles is 8°. In a collision of this kind, the vehicles are deflected back satisfactorily without the occupant being exposed to harmful deceleration and without other traffic being seriously endangered.

The following brief observations may be made on this type of lateral clearance:
— the width of the traffic lane tube does not show a significant increase in comparison with the traditional solution using footways, and the tunnel construction costs are therefore practically the same;
— the traffic safety is increased because there are no elevated obstacles with a height of more than 5 to 7 cm immediately next to the traffic lane;
— vehicles which swerve off course have a strong likelihood of being deflected back in a satisfactory manner;
— the distance between the traffic lane and the wall is 1.15 m (including the painted lane markings on the road surface with a width of 0.15 m). In this connection, it should be noted that a distance of 1.00 m is considered a minimum for the purpose of traffic flow. It may be necessary to increase the width of 1.15 m in the case of tunnels with substantial horizontal curvature in order to guarantee the stopping-sight distances. This is the case with the Drecht tunnel where the radius of horizontal curvature is 800 m. Here the distance between the wall and the traffic lane has been increased to 2.10 m. This widening is of course only possible on one side, i.e. the side of the lane situated towards the centre of the circle;
— the level strip may be used for pedestrians (maintenance and emergency situations), provided that the adjacent traffic lane is closed by means of the signals. In all probability, the safety is then greater than in the case of the solution widely adopted abroad, i.e. a low footway without signals.
Clearly continuous supervision (remote or otherwise) of the tunnel is essential in this case.
In the draft directives of the Rijkswaterstaat [lit. 10] illustrated in figure 3, the headroom above the traffic lanes is 4.50 m and above the level strips 4.20 m. The value of 4.50 m is maintained not only in tunnels but also under civil engineering works above motorways. The maximum permitted height of vehicles using these motorways is 4.00 m. The lower height above the level strips is permissible because vehicles are only stationed there exceptionally.
In the older tunnels a headroom of 4.20 m was adopted corresponding to the then maximum permitted height of vehicles of 3.80 m. No limitations are placed on the height of vehicles using these tunnels at present. This means that commercial vehicles with a height of 4 m can also use such tunnels. As the margin has become very small (0.20 m), horizontal wires have been fitted at the approaches to the Velser, Coen and Benelux tunnels at a height of 4.13 m above the carriageway. When these wires are touched, the red traffic lights in front of the tunnel are switched on. This happens three or four times a week at each of the tunnels, corresponding roughly to 1 in 100,000 vehicles.

Despite these measures, the ceilings and equipment fitted above the carriageway are regularly damaged; the damage is often due to flapping tarpaulins on lorries. It must also be remembered that a moving commercial vehicle acquires a vertical oscillation due to irregularities in the road surface. In Germany it has been observed that this movement may result in deviations of 0.20 m above the level of the stationary vehicle.
In the Heinenoord tunnel where the vertical clearance is 4.50 m, damage is extremely uncommon, although the underside of the booster fans mounted at this height above the carriageways shows some scratches, probably caused by flapping tarpaulins.

The above observations show that a clearance of 0.50 m above the maximum permitted vehicle height is certainly not a luxury.
Over and above this a space of 0.35 m is often allowed; this is sufficient to install the lighting fittings and cross-arrow signals. The acoustic ceiling (with a thickness of 0.07 m) is interrupted at the location of these installations so that the full 0.35 m is available for them.
We thus arrive at the following principal dimensions for the traffic tubes:
For a two-lane carriageway, the width between the walls is 9.40 m and for a three-lane carriageway, 13.00 m. In both cases, the minimum height from the top of the road surface to the base of the tunnel roof is 4.85 m. Above the level strips this may be reduced to about 4.30 m (4.20 m clearance and approx. 0.1 m acoustic ceiling) based on the assumption that no fittings are mounted above the level strips.
The carriageways are often given a minimum camber of 1 : 60 to drain off water. This value is to some extent arbitrary as on the one hand there is no precipitation and on the other the longitudinal gradient greatly predominates in most cases. In the Coen tunnel where no camber at all has been provided, this has not led to unsatisfactory results (puddle formation). Despite the absence of precipitation, water is still present in tunnels: the walls are regularly washed and vehicles themselves introduce humidity, while — although the aim is watertightness — some leakage water is practically unavoidable.
A service gallery (fig. 1) is often provided between the traffic tubes each of which contains one carriageway of the motorway; this corridor is linked to the carriageway tubes by doors at intervals of 90 to 100 m. At the two ends of the enclosed tunnel section this gallery is accessible by stairways.
The central gallery has a number of functions:
— it is used to house the electrical cables for the tunnel equipment (lighting, signals, pumps etc.), the fire mains and the piping for the pump situated at the lowest point of the tunnel;
— maintenance staff can reach any required point in the tunnel by means of this gallery without having to remain for too long in the noisy traffic tubes which often also have a high fume level.
It should be noted, however, that maintenance personnel are increasingly using

service vehicles which provide extra protection during working activities if they are equipped with flashing lights and parked above the point at which work is necessary.
— in the event of a disaster (fire etc.) the gallery can be used as an escape route;
— in some cases (Benelux and Coen tunnels) the gallery forms part of the ventilation system (see 2.1.2).

To ensure accessibility, the gallery should have a width of at least 1.25 m. The height is derived from the height of the traffic tubes and the necessary floor and roof thickness. A greater width is only necessary for very long tunnels (housing cables and mains) or if the gallery is also used for ventilation purposes.
In some short tunnels (Heinenoord and Dordtsche Kil) the central gallery has been omitted and cables and mains are installed in the traffic tubes.

2.1.2 *Ventilation requirements*

Internal combustion engines generate gases, some of which are unpleasant or harmful to human beings. In a tunnel the ventilation system must keep the concentraion of these gases below acceptable values by 'flushing out' with fresh air. A distinction may be made between the following systems:

A NATURAL VENTILATION in the case of which a longitudinal air current is generated in the traffic tube through the impulse effect of moving vehicles (Vlake tunnel).

B ARTIFICIAL VENTILATION:
1 *Longitudinal ventilation by injection.* At the beginning of the traffic tube, air is blown into the tube through a slit in the roof at high speed in the direction of traffic movement, thus increasing the natural longitudinal flow (Coen and Benelux tunnels).
2 *Longitudinal ventilation with booster fans.* Booster fans are suspended in the traffic tubes above the headroom or against the walls above the footways; these fans intensify the longitudinal air current created by the vehicles (Schiphol, Heinenoord and Drecht tunnels).
3 *Transverse ventilation.* Separate ducts are provided in the cross-section to supply fresh air and extract contaminated air. The ducts are connected to the traffic tubes by openings. The fresh air is often introduced into the traffic tube from below and extracted from above (Maas, Velsen, Y tunnels).
4 *Semi-transverse ventilation.* A duct is provided in the crosssection for the supply of fresh air. Through openings, the air emerges into the traffic tube, thus creating over-pressure so that the contaminated air flows off towards the ends of the traffic tube. The direction in which this occurs depends on the position in the tunnel, the speed and density of traffic and the wind pressures at the tunnel portals.
This system is used for auxiliary ventilation in the Coen and Benelux tunnels. For normal conditions, longitudinal ventilation is provided here. Longitudinal ventilation

is, however, less suitable if traffic moves in two directions in a single tube; this may be the case in the event of extensive maintenance work or a serious accident in the other tube. For this purpose, in the case of these two tunnels the central gallery is dimensioned in such a way that it can be used to supply fresh air for semi-transverse ventilation of one of the traffic tubes. Adjustable valves in the openings make it possible to supply the left or righthand tube.

It is not possible to indicate the influence of each of these systems on the geometry of the cross-section. Too many factors are involved here such as the composition, speed and density of traffic, the length of the tunnel tube, longitudinal gradients, number of traffic lanes etc. A responsible choice of the ventilation system and the corresponding dimensions can only be made or determined in a concrete situation on the basis of an economic study taking into account civil engineering and electrical and mechanical engineering investments and operating costs. A few considerations are set out below concerning the choice of system and influence on the cross-section.

A Natural ventilation has no influence on the cross-section but can only be used in relatively short tunnels. The maximum length is between 300 and 350 m if the traffic tubes are used exclusively in one direction.

B.1 *Longitudinal ventilation with injection.* This system has no influence on the cross-section. Here again, however, there is a limitation on length. The longer the tunnel the greater the resistance in the tunnel tube (filled with vehicles) so that more air will escape towards the upstream tunnel portal located close to the injection opening. This air is lost for ventilation purposes. In the Coen tunnel with a length of 587 m normal injection ventilation could be used but in the case of the Benelux tunnel with a length of 795 m, the injection had to be reinforced by booster fans suspended in the traffic tubes. Both tunnels have two traffic lanes per tube.

B.2 *Longitudinal ventilation with booster fans.* This system will generally influence the cross-sectional geometry unless the fans can be accommodated above the footways; this is only possible when the number of fans is limited (short tunnels).

As stated in section 2.1.1 an extra height of 0.35 m is available above the headroom. In the Netherlands fans are generally used with a diameter of 0.65 m; with the fan casing and mountings a height of 0.85 m will be necessary. This corresponds to an increase in the tunnel height of 0.50 m. In the case of longer tunnels it may be desirable to use fans with a wider diameter to obtain a more economical solution.

One of the limitations on use is the longitudinal air speed which is considered to be acceptable to traffic without creating an obstacle. If a value of 10 to 12 m/sec is taken for this speed, tunnels with a length of 2 to 2.5 km can be provided with booster fan ventilation. All the tunnels now under construction or projected in the Netherlands are equipped with this economically attractive ventilation system, including the 1980 m long tunnel under the Westerschelde.

B.3 *Transverse ventilation.* In the previous systems the traffic tubes themselves are used to convey air. In this case, however, extra ducts must be provided for the supply and extraction of air. This means a considerable widening of the tunnel cross-section although higher air speeds are acceptable in the ducts than in the traffic tube. The application is not limited by the length of the tunnel. Because of the relatively high costs this system is at present considered less attractive for the fairly short tunnels built in the Netherlands.

B.4 *Semi-transverse ventilation.* Compared with transverse ventilation, half the area of air ducts will be sufficient as the traffic tube is used for extraction purposes. This means that there is a limit on application as a function of length, as in the case of longitudinal ventilation with booster fans. In the Netherlands, this system has only been used for auxiliary ventilation of the Benelux and Coen tunnels.

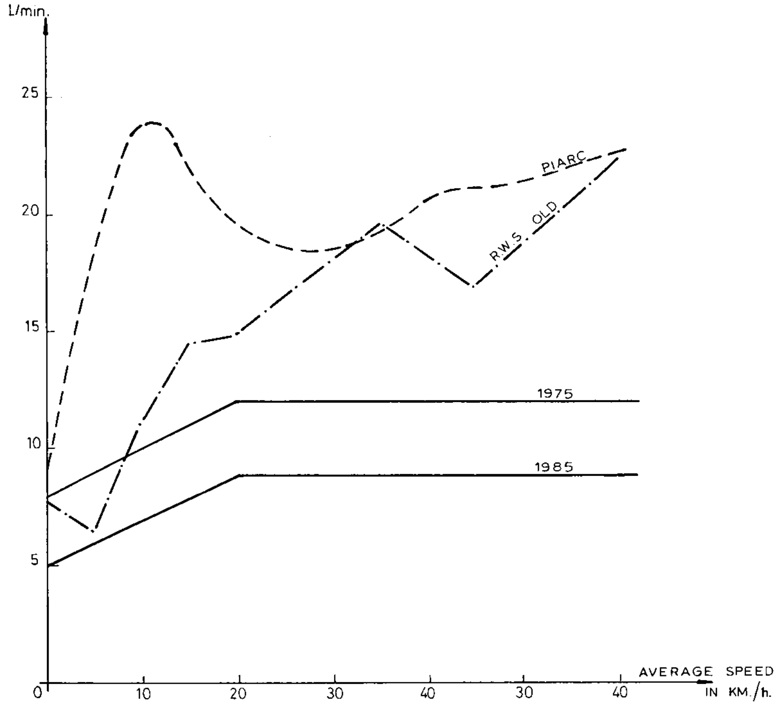

Figure 4. Volume of CO emitted by an average passenger car expressed in litres per minute.

Without dealing exhaustively with the subject of ventilation, it seems interesting to look briefly at a new development in the area of vehicle exhaust gases relating in particular to the generation of carbon monoxide (CO). Up to now, CO emission has been the decisive factor in the design of ventilation. The quantity of CO generated in a tunnel is equal to the product of the number of vehicles present in the tunnel

and the emission from an average vehicle. Both these factors depend on speed. Figure 4 gives a number of graphs for the relationship between CO generation by an average private car and average speed. Especially at fairly low speeds, the average speed is obtained from a cycle consisting of stationary periods, acceleration, braking etc. The curve followed by the Locks and Weirs Department and based on Swiss and German data is marked RWS (old). The P.I.A.R.C. curve was published by the P.I.A.R.C. Road Tunnels Committee in its report to the World Road Congress in 1971. The values based on French measurements in 1969 are relatively high. This is one of the reasons why the Tunnel Engineering Section of the Netherlands Royal Institute of Engineers has set up a study group on road tunnel ventilation.
The TNO Institute for Road Transport, represented in the study group, has plotted, on the basis of measurements and studies, curves for 1975 and 1985 representative of the average private car driven on Netherlands roads in those years. The lower emission values result in part from the stricter regulations which have been and will be introduced in respect of the exhaust gases of new cars.
This reduction in CO emission makes it necessary to give greater attention to the generation of fumes by diesel engines in the design of tunnel ventilation systems. Experience has shown that if ventilation is based on the 'old' CO generation and on a permissible CO concentration of approximately 150 ppm, the deterioration in visibility resulting from the generation of fumes by diesel engines remains within acceptable limits.
With the new CO emission values, it is not inconceivable that visibility may become the criterion for the necessary quantity of fresh air, especially in tunnels where diesel trucks represent a large percentage of the overall traffic. The Road Tunnels Committee referred to above published a recommendation in 1975 on a method of calculating the deterioration in visibility, including limit values to be observed [lit. 23].

2.1.3 *Constructional requirements*

The previous section dealt with the 'hollow spaces' which must be created in the tunnel. Closer attention will now be given to the dimensions of the surrounding solid sections, i.e. the reinforced concrete structure. These observations are confined to immersed tube tunnels made of concrete.
In the process of construction, two stages are important: floating transport and the final phase.

The tunnel elements which generally have a length of about 100 m are manufactured in a building dock which can subsequently be flooded with water. The elements are then floated to the point at which they must be immersed. At this stage, the element is provided with a temporary watertight bulkhead at each end and the necessary immersion equipment (directional towers etc.). The clearance above the water is generally 5 to 10 cm which, with the normal (external) tunnel height of about 8.0 m, means that the gross content multiplied by the specific weight of water exceeds the weight by about 1%.

The element is then sunk by means of temporary ballast (often water); at a later stage, the temporary ballast is replaced by definitive ballast in the shape of non-reinforced concrete in the traffic tubes below the carriageway to be built later. The immersion equipment and end bulkheads have been removed in the meantime. The element must now have a sufficiently greater weight than its floating capacity for it to remain in place. In this connection, the pressure head of the ground water below the tunnel base may lag behind the water level in the (tidal) river. At low tide, this may result in an additional upward force. To compensate effects of this kind, the design criterion is often adopted that at this stage the weight of the tunnel must exceed the water displacement by about 600 kgf per m^2 tunnel base corresponding to an additional allowance of 7.5% for an external tunnel height of 8 m. The safety margin is later increased because the dredged trench in which the tunnel is immersed is filled in again. This results in the first place in friction on the walls but also in a load on the roof. Depending on the longitudinal section of the tunnel and the cross-section of the waterway, the latter factor may be very slight in places or even disappear altogether due to erosion of the river bed.

Assuming that, in cross-sectional terms, the surface area of the hollow space is V m^2, that of the structural concrete C m^2 and that of the ballast concrete (including the carriageway) B m^2, the following two equations can be written (see also fig. 1):

In the transport stage:
Weight = 0.99 water displacement, or

$$2.49 \times C + 3.0 = 0.99\,(V + B + C) \tag{1}$$

In the final phase:
Weight = 1.075 water displacement, or

$$2.46 \times C + 2.25 \times B = 1.075\,(V + B + C) \tag{2}$$

The following points should be noted in connection with these equations:

— A value of 2.49 has been taken as the specific weight of reinforced concrete in equation (1) and a value of 2.46 in equation (2). Experience in the Netherlands has shown that safe working limits will be obtained if it is assumed that the specific weight of concrete (without reinforcement) varies between 2.36 and 2.39 tf/m^3. This dispersal range not only allows for variations in the specific weight of concrete (which generally fluctuates around a mean value of approx. 2.375 tf/m^3) but also for dimensional deviations in the concrete structure (e.g. thicknesses of structural components) in relation to the theoretical dimensions shown on the drawings. The high specific weight has been taken in the floating state and the lower weight in the final situation. The calculation also allows for 140 kg structural and reinforcing steel per m^3 concrete.

— The surface area of the ballast concrete has been multiplied by a specific weight of 2.25 representing the weighted mean of 0.50 m concrete with a specific weight of

2.3 (the compression of ballast concrete is generally less good than that of structural concrete) and 0.07 m asphalt road surface with a specific weight of 2.0.
— A weight of 3.0 tf/m' has been introduced in equation (1) for the immersion equipment and end bulkheads.
— In the equations it has been assumed that the specific weight of water is 1.0. This must be checked in each individual case. In a tidal river it is quite likely that a value of 1.0 must be taken for equation (1) and a higher value for situation (2) resulting from the salt strip penetrating in along the river bed.
— A number of mean values have been used in the equations. This means that in specific cases more accurate data must be used, e.g. for the quantity of reinforcing and structural steel, the dimensions of recesses, the shape of the element and sections, the immersion equipment and end bulkheads etc.

Solution of the equations gives the following results (in m^2):

$$C = 0.711\ V - 1.1 \qquad (3)$$

$$B = 0.077\ V + 1.3 \qquad (4)$$

Solution (3) is particularly important because it shows the relationship between the available surface area for constructional purposes and the hollow space which must be taken as the starting point for the design. The surface area V is the sum of the required traffic clearance profile and the surfaces needed for maintenance, equipment and ventilation as described in sections 2.1.1 and 2.1.2.
The structure must be strong enough to withstand in the final phase the loads due to water and ground pressure and its own weight, taking into account the stresses caused by temperature changes.
In the case of tunnels built up to now in the Netherlands, it has been found that with the surface area calculated from (3), a reinforced concrete structure of sufficient strength can be built. The deepest elements of the 2 × 2 lane Benelux tunnel were an exception to this rule; here allowance had to be made for a water pressure of almost 21.0 m on the roof. In this case the floors and roof sections were partly prestressed in the transverse direction.
If a greater surface area is required than suggested by equation (3) due to a great depth or width of the traffic tubes, a choice must be made between the following solutions:

a Total or partial transverse pre-stressing of the tunnel; in this way a lower structural height will be sufficient than with reinforced concrete.
b Use of lightweight concrete for the entire cross-section or parts thereof (e.g. roof and floor sections).
c Increase in the hollow space V. This may be favourable for ventilation purposes.

The final choice must of course be made on the basis of an economic study taking into account both capital investment and operating costs (ventilation).

In conclusion, a few general remarks appear desirable.
In the case of roof and floor sections, the decisive factor will generally be shear forces and not the bending moments. Therefore, the structural elements do not generally have a constant thickness but are reinforced towards the walls.
In the case of most immersed tube tunnels (fig. 1) a bevelled section with a height and width of 1.50 m will be found in the two top corners of the cross-section. At the base this bevel has a circular shape. This shape has been chosen to prevent dragging anchors gaining too easy a grip on the tunnel and — in particular — damaging the watertight lining. It should be remembered in this connection that most tunnels only have a shallow covering of earth wich may disappear altogether close to the edge of the channel (transition between bed and embankment). Tunnels are intentionally laid at a shallow depth for greater economy.

2.2 Longitudinal profile

2.2.1 *Traffic and maintenance requirements*

Since the construction of the Benelux tunnel, the following norms have been observed for motorway tunnels:

— Maximum gradient: $4\frac{1}{2}\%$
— Minimum radius of base curvature (concave): 2,500 m
— Minimum radius of upper curvature (convex): 10,000 m.

Where the width and water depth of the channel to be crossed are often a fixed initial parameter for the tunnel design, the choice of gradients and radii determine in large measure the length of the tunnel. Shallow gradients and wide radii make for an expensive tunnel. On the other hand these parameters must be fixed in such a way that the levels of service in the tunnel coincide as far as possible with those for the road as a whole.
A study carried out in 1962 by the Locks and Weirs Department showed that for gradients in the order of 3 to 5% it is desirable to provide crawler lanes for uphill traffic (trucks) if the height difference to be overcome exceeds about 10 m. The initial assumption here is that the speed of a truck with an engine capacity of 6 HP per ton of weight should not drop below 40 kph if the gradient is appoached at a speed of 60 kph. Since then tunnels have been provided with a crawler lane on the upgrade in the open access sections in the waterway banks.
The provision of this extra lane in the immersed section would result in very high costs. In the Netherlands the maximum gradient from the deepest point to the start of the section to be constructed on the bank is fortunately often less than 10 m.

Experience of these tunnels with their gradients which are unusually steep for Netherlands conditions is favourable. As an example, in the Coen tunnel an hourly traffic density of some 4,300 vehicles per two lane traffic tube is recorded several times each week. The difference in height between the lowest point under the channel and the road outside the tunnel is here a good 23 m and the maximum gradient is 3.5%.

It seems that in practice lorries make little use of the crawler lanes which are not compulsory. This may be due to the drivers' fear that it will be difficult for them to rejoin the traffic on the normal carriageway at the end of the lane.

The Traffic Engineering Department is at present examining the extent to which use is made of crawler lanes and, more generally, the influence of tunnel gradients and crawler lanes on traffic flow.

At the time of writing the results of this study, carried out at the Heinenoord tunnel with maximum gradients of 4.5%, are not yet known.

Table 2 shows that the influence of gradients on tunnel costs is not inconsiderable.

Table 2 *Influence of gradient on tunnel costs (in millions of guilders)*

1	2	3	4	5
Gradient %	Depth	Extra cost as against 4½% tunnel due to greater length	Extra cost if crawler lane provided	Total columns 3 & 4
2	Shallow	13.6	—	13.6
	Deep	21.7	—	21.7
3.5	Shallow	2.1	1.6	3.7
	Deep	4.95	2.15	7.1
4.5	Shallow	—	1.3	1.3
	Deep	—	1.45	1.45

The table relates to 2 × 2 lane tunnels. A deep tunnel is defined here as one in which the difference in height between the road surface at the deepest point and the road surface on the adjoining road is 25 m. For a shallow tunnel, a value of 18 m was taken. The costs relating exclusively to the civil engineering works and not to the adjoining road are naturally very approximate. According to normal practice it was assumed that crawler lanes are necessary for gradients steeper than 2% but not below this value.

Reference has been made above exclusively to the maximum gradients which are determined by traffic requirements on the one hand and costs on the other. In the case of tunnels which cross a broad waterway (e.g. the proposed Westschelde tunnel with a length of 1,980 m for the tunnel proper), the deepest section may be laid

horizontally for simplicity. However, there is the important operational requirement that any leakage and washing water must be drained to the lowest point where there is a pumping station. For this purpose, the longitudinal section has a minimum gradient of about 0.4%.
Like the maximum gradients, the radii of curvature also determine to a great extent the cost of a tunnel. They should therefore be smaller than is normally the case for motorways in open country. But they are chosen in such a way (base 2,500 m, top 10,000 m) that the stopping sight distance and traffic comfort are ensured.

2.2.2 *Transition from closed to open construction*

A distinction can be made between the following tunnel sections:

a The closed section, sub-divided into:
  1 the immersed tube tunnel;
  2 the abutments which are built in the banks immediately in front of the immersed tube tunnel section and above which — if necessary — the ventilation shafts and buildings can be constructed. If no shafts are needed, a length in the order of 15 to 20 m will be sufficient.

b The open approaches which, together with a 2, are constructed in cuttings on the banks.

The location of the transition from a to b is determined by economic considerations in which the following points come into play:
— The desirability of making the closed section as short as possible for ventilation reasons. Emission and the quantity of air which is therefore needed increase on a linear basis with length; the same applies to air speed (in the case of longitudinal ventilation) so that the necessary fan capacity increases approximately by a power of 2.
— Under normal conditions, the point at which the cost of the civil engineering works for a closed structure built locally is equal to the cost of an open through structure will be reached when the road is 12 to 14 m below the ground surface. At shallower depths an open structure will generally be less expensive.

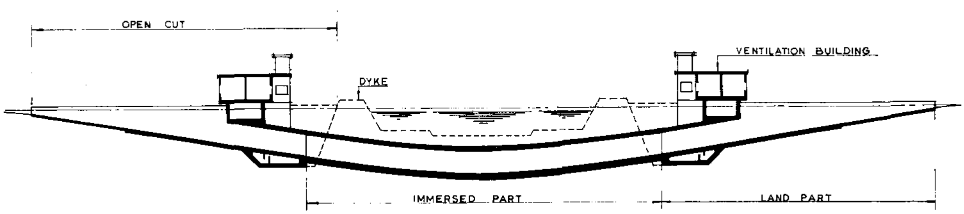

Figure 5. Longitudinal section.

These considerations often lead to the type of design shown in fig. 5: the head of the cutting in which the sections on land are built consists of an embankment directly behind the existing dyke. The closed abutment on land (20 m or as long as is necessary for the ventilation building) is constructed at the deepest point of the cutting with the open approach on its landward side. In this way, expensive structures at the end of the cutting (cofferdams etc.) are avoided and a short closed tunnel obtained. Special circumstances may make it necessary to depart from the method described above, e.g. intersections with road and rail routes and ground water level requirements (avoidance of drainage pump systems during construction in the event of poor soil characteristic and vulnerable structures).

3 Some aspects of design and construction

3.1 General description of tunnel construction

The construction of immersed tube tunnels has already been described in detail on several occasions [lit. 3 to 7]; only the main features will therefore be outlined here. For the immersed section, elements with a length of 90 to 125 m are built in a construction dock (photos 1 to 3). The two ends of each element are provided with temporary watertight bulkheads (end bulkheads) so that hollow containers are obtained which can be floated (photo 4). Once the work in the dock has been completed, it is flooded with water and the dyke between the dock and waterway is dredged open. The elements are then towed to the immersion trench dredged meanwhile in the waterway between the two land sections and sunk by applying ballast (usually

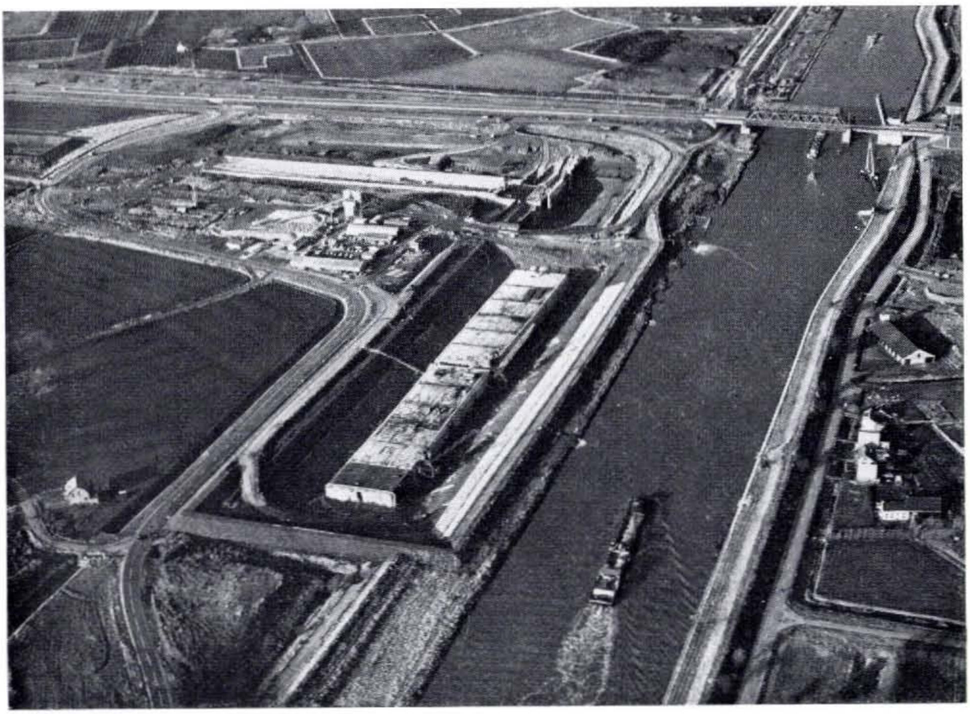

Photo 1. Vlake tunnel; the two tunnel elements in the building dock are almost completed; in the background: one of the open approaches under construction.

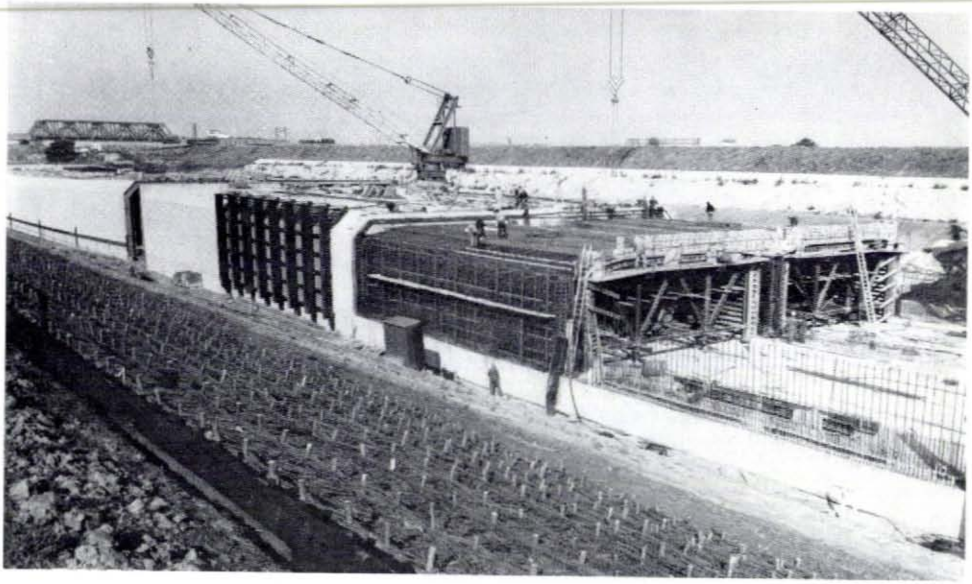

Photo 2. Vlake tunnel; constructing the two tunnel elements in the building dock.

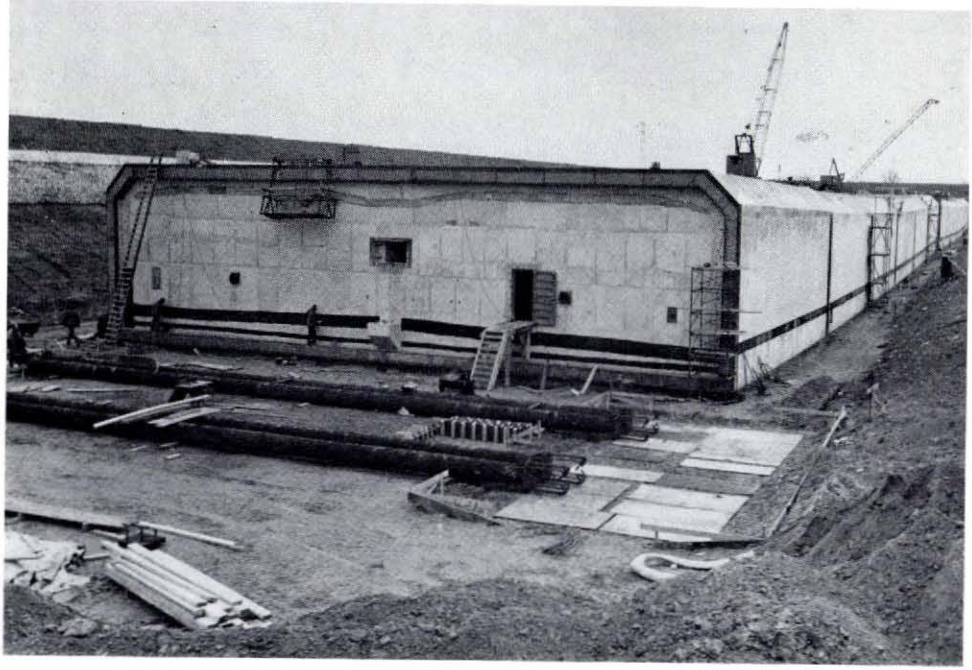

Photo 3. Vlake tunnel; the two elements are almost completed and provided with (concrete) end bulkheads.

temporary water ballast). The connection between the first element and the land section, and also between the individual elements, is effected as follows (see figure 6). The element which is brought into position during the immersion operation and held by six horizontal warping cables and four vertical cables (from the pontoons located above the element), is placed on the bed on three temporary supports with its end surface at a distance of about 0.10 m from the previous element. The position and elevation are determined during the manoeuvre through the two temporary directing towers which have shafts so that the inside of the element is accessible from the water surface.

Photo 4. Vlake tunnel a floating tunnel element with pontoons and directional towers.

One temporary support consists of a 'locating' attachment on the previous element and the two others of concrete slabs placed on the river bed close to the free end. The element rests on these slabs through vertical jacks allowing height correction. The element is then drawn up against the previous element and the soft tip of the rubber Gina section is compressed. This section is fitted on the entire periphery of the element end. In this way a water-filled chamber is obtained between the two end bulkheads and inside the Gina. When a valve in one of the end bulkheads is opened, water flows out of the chamber so that the water pressure ceases to exist here but remains present at the free outer end. The hydrostatic pressure is so great that the element is pressed further against the previous element and the Gina com-

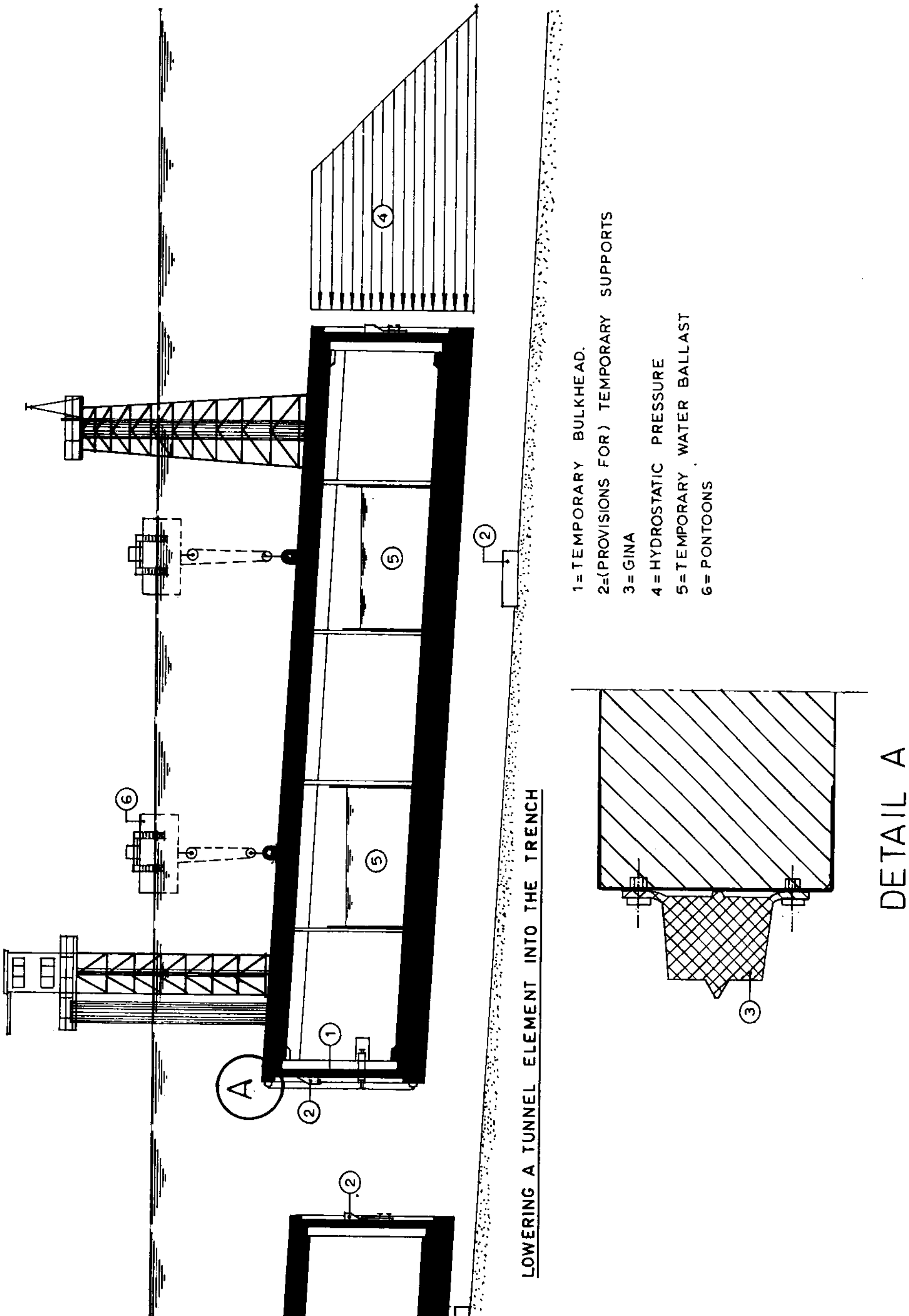

Figure 6. Lowering a tunnel element into the trench.

pressed to such an extent that a good water seal is obtained. If necessary, horizontal correction of the free outer end can be effected with horizontal jacks. In the case of the Drecht tunnel these jacks are located in the space between the two elements as far as possible excentrically in the horizontal plane. By pumping up the jacks, the pressure on the Gina section is relieved at one side and the element can be slewed horizontally.

It is only when the connection is established between the last two elements that water pressure cannot be used. This sealing joint with a width of approx. 1 m, allowing the final element to be positioned between the two adjacent elements, is sealed on the outside by watertight bulkheads which are fitted by divers. The water is pumped out of the joint and the final structure completed on the inside under dry conditions. Before fitting the watertight bulkheads, wedges are placed in the sealing joint to prevent the two elements moving towards each other on either side while pumping dry (the Gina sections in the normal immersion joints are still under tension while the reaction on the bulkheads at the sealing joint ceases).

The tunnel rests in the first instance on the jacks. A layer of sand is now jetted between the base of the tunnel and the bed of the dredged trench. In the case of earlier tunnels, this was done with the aid of a gantry travelling on the tunnel roof with the jetting and intake tubes secured to it. A different method is to be applied on a large scale for the first time at the Vlake tunnel where the sand and water mixture will be washed under the tunnel from the tunnel tube through openings in the base which can be closed [lit. 7 and 12]. This new patented method of applying the sand has the advantage that the obstacle to shipping (created by the gantry) is eliminated. After applying this layer of sand with a thickness of 0.5 to 1.0 m, the jacks are lowered and the tunnel has a uniform support. The rest of the trench is filled by dumping earth from the water surface. In some cases it may be necessary to support the tunnel on piles; descriptions of these operations will be found in literature 6 and 8. It now remains to remove the end bulkheads, apply the layer of ballast concrete within the tunnel section (see 2.1.3.) and remove the temporary ballast (tanks). At the immersion joints, a second seal is fitted within the Gina barrier consisting of a canvas-reinforced rubber section which is bolted onto the concrete structure. At the location of the immersion joints, a dowel structure is also fitted by means of which uneven movement perpendicular to the tunnel axis can be prevented when the elements are connected together.

To prevent continuous cracks forming in the concrete structure (waterseal), the immersion joints are not only designed flexibly but the elements are also subdivided into sections with a length of approx. 20 m each, connected together by expansion joints. To ensure a water seal, rubber-metal strips are inserted in the joints while on the outside surface, in the case of lined tunnels, the watertight lining is continued and in the case of unlined tunnels, a polyurethane water seal is applied (fig. 7).

The construction of the tunnel in longitudinal sections with a length of approx. 20 m prevents excessive tensile stresses due to temperature changes, shrinkage and uneven

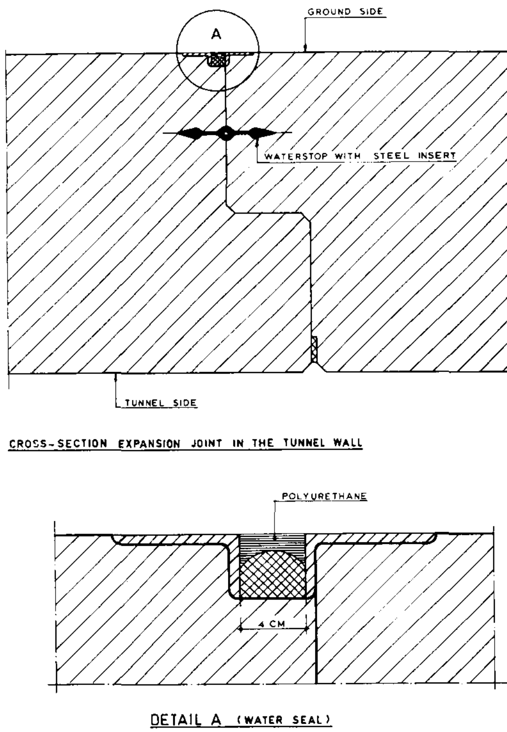

Figure 7. Cross-section of expansion joint in the tunnel wall.

settling of the sub-soil. The latter is particularly likely to occur close to the joint with the sections built on land which often have pile foundations. The expansion joints are therefore designed in such a way that they prevent uneven movement of the sections in relation to each other, perpendicular to the longitudinal axis (thus there will be no factures in the road surface etc.), while allowing a reduction or increase in the length of the sections (shrinkage, temperature changes) and rotation of the sections in relation to each other. Thus the tunnel can follow uneven settling of the subsoil like a chain without the occurrence of excessive stresses. During transport and immersion, a temporary longitudinal post-tension system ensures that the sections which together form an element, act as a single unit. The post-tension is removed once the sand foundation has been applied.

Simultaneously with the construction activities in the dock, the land sections are built in open excavations on the two banks (photos 5 and 6), i.e. the closed section which forms the abutment for the immersed part (provided if necessary with the ventilation shaft and buildings) is at the lowest point, adjoining the reinforced concrete trough profile which forms the open access route. This structure is continued until the road surface reaches a level approximately 1 m higher than the highest ground water level. During the building work, the excavations are kept dry by means of well points.

Like the immersed elements, the end of the land section is provided with a temporary watertight bulkhead. Behind the existing dyke (fig. 5 and photo 1) a second dyke is provided; it is connected to or laid over the land section of the tunnel. The existing water barrier is then dredged through, the immersion trench dug and the elements sunk into position adjoining the land section.

The general method of tunnel construction has been outlined above. Local conditions may make a different solution necessary or more desirable economically.

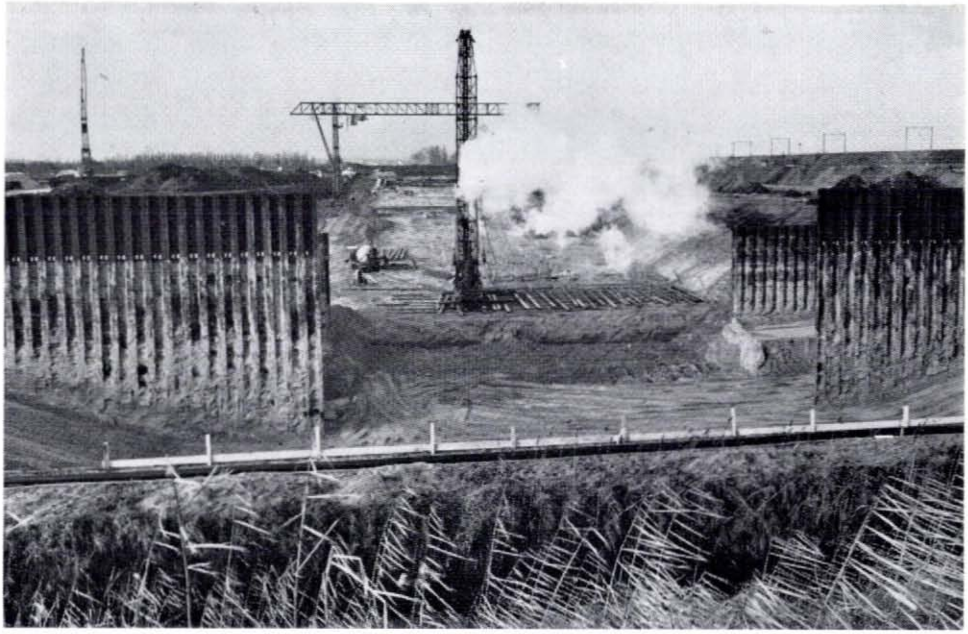

Photo 5. Vlake tunnel; cutting for one of the approaches. The tension piles are being driven. In the foreground: the steel sheet piling which will subsequently form the cofferdams, joining the new dyke to the tunnel.

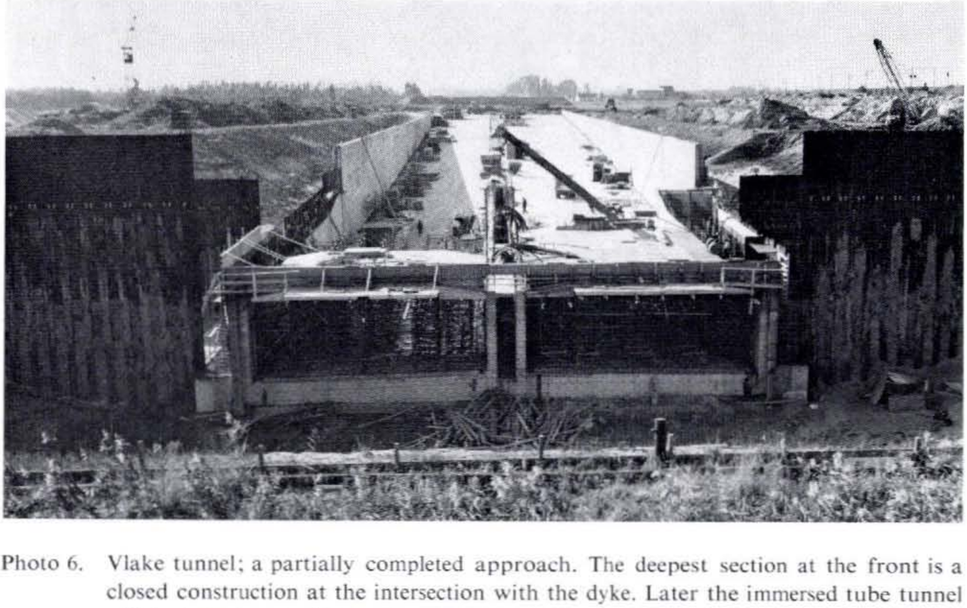

Photo 6. Vlake tunnel; a partially completed approach. The deepest section at the front is a closed construction at the intersection with the dyke. Later the immersed tube tunnel will be joined up to this section.

The Margriet and Drecht tunnels now under construction are examples of this. In the case of the Margriet tunnel, the designers faced the following problem. The tunnel element ($77 \times 28.3 \times 8$ m) was both too deep and too wide to be transported on the canal (canal depth 4.0 m). Here instead of being built in a construction dock, the element is manufactured in one of the open approaches which is locally widened somewhat for this purpose. On completion of the open approaches (the land sections consist exclusively of reinforced concrete trough structures) the dykes between the construction site and the canal are dredged open and the immersion trench dug. The ends of the approach sections are not provided with temporary bulkheads; this means that during this phase the approaches are also filled with water. The element is now floated out of the approach section and immersed into position. The watertight joint at the two approach sections is not obtained with the Gina section but by means of a rubber tyre inflated between the concrete of the element and the concrete of the approach section. Once the water has been pumped out of the approach, a definitive seal is installed behind this temporary seal.

The Drecht tunnel with its 4×2 traffic lanes and an external width of 49.04 m is a giant among immersed tube tunnels. As the tunnel is built in the urban areas of Zwijndrecht and Dordrecht and the subsoil is of poor quality, well points are not permitted in order to prevent damage to buildings. This presents no problem for the construction of the three immersed tube elements with a length of approximately 115 m: the construction dock is located at a distance of 12 km from the tunnel site. However, a different construction method had to be adopted for the land sections which are normally built in open cuttings.

For the open approaches an impermeable layer of clay was fortunately found at sufficient depth in the subsoil. A start was made by driving walls of steel sheet piling reaching down to the clay layer around the approach. Within this invisible waterproof enclosure (sheet piling plus clay layer) an excavation was now made with the necessary depth to build the road (fig. 8). The enclosure has a permanent function as in this case there is no need to build the normal concrete through structure.

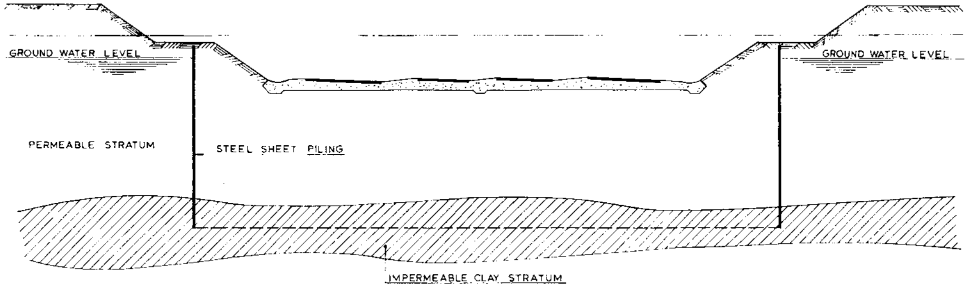

Figure 8. Open approach of the Drecht tunnel.

The closed land sections built in the banks each have a length of about 110 m. This unusual length is needed because of intersections with road and rail routes in this urban area and the phasing of road diversions during the building work: traffic must not be interrupted while the tunnel is being built. The design was determined by two requirements: no well points and availability of the surface again as soon as possible (roads etc.). These two factors led to the use of the so called wall-roof method (fig. 9). From the surface, diaphragm walls are sunk down to the impermeable clay layer and piles are driven at the position of the partition walls.

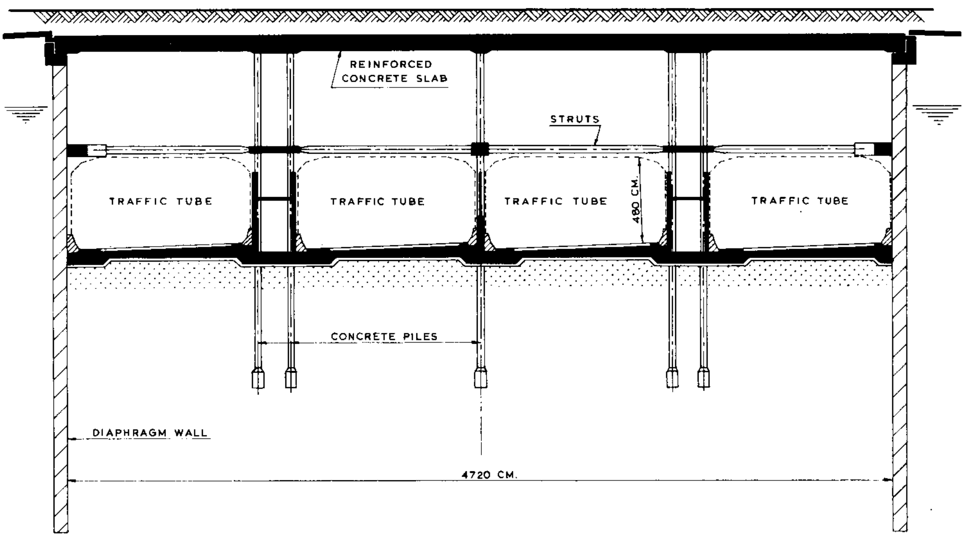

Figure 9. Cross-section of cut and cover part of the Drecht tunnel.

A reinforced concrete roof slab is subsequently built on the surface which is then available again for road and rail traffic while construction work on the tunnel continues below the slab. The soil is removed down to a given depth after which horizontal struts are fitted between the diaphragm walls in order to limit the bending moments in them. The soil is then excavated down to the level of the base of the future road and a concrete floor is laid here. It remains to build the actual tunnel tubes with a road surface and partition walls consisting of panels which must hide the piles at the tunnel walls and the diaphragm walls; a ceiling also has to be built. The space above the traffic tubes and below the roof slab is used locally as a service area.
Each of the 'wall-roof' sections is built in two units with a length of approx. 55 m so that even during construction one section is available for intersecting road and rail traffic etc. The diaphragm walls and the impermeable clay layer endure that the ground water level in the vicinity is not lowered.

3.2 Waterproof concrete instead of waterproof lining

3.2.1 *Introduction*

In the Netherlands, practically all tunnels run under waterways, while all tunnels and the majority of underpasses and roads in cuttings are exposed to ground water pressure. Leaking floors, walls and roofs make a slovenly impression; the attachment of the carriageway to the support base may be broken by water pressure; the walls become dirty thus reducing brightness (lighting !); puddles on the carriageway are dangerous especially in winter (sudden icing); reinforcing elements may be damaged etc. To remedy these problems all tunnels were given a waterproof lining until recently.

What is in fact the real likelihood of leakage? Concrete with a thickness of several decimetres is in itself waterproof, provided that it is properly prepared and worked. There are many capillaries in concrete but they are not all linked up. This can be investigated by means of water penetration tests in which concrete prisms are exposed several times to water pressures up to seven atmospheres. By splitting open the prisms, it is possible to see how far the water has penetrated in by examining the colouring. For good quality concrete the maximum penetration is 5 cm.
The risk of leakage increases if there are cracks extending over the entire thickness of the concrete. In many tunnel walls, cracks running over 3 to 6 m will be found. They extend from a few centimetres above the floor up to the ceiling and may have a width of 0.4 mm.
The waterproof lining must therefore be able to bridge these cracks and at the same time resist the water pressure.
The waterproof lining may consist of steel plates or one or more flexible layers (rubber, bituminized fabric or plastic materials).
Application of the lining is a difficult and time-consuming operation and it is often only possible to work under particular weather conditions. Frequently the lining itself must be provided with a protection against mechanical damage or against stripping through friction with the soil etc. In short a waterproof lining is expensive.

3.2.2 *The causes of cracking*

As mentioned above, cracks occur primarily in the walls. They form when the tensile stresses are so high that the tensile strength of the concrete is exceeded.
If there are no external stresses, stresses may occur simply as a result of physical phenomena, the most important being: temperature characteristics, shrinkage and creep.

TEMPERATURE CHARACTERISTICS
Heat is produced when concrete sets. In the case of thin structural elements this

heat flows off directly through the shuttering to the ambient air, but if the structural elements are thick more heat is produced than can be conducted away so that the temperature of the concrete rises.
In 1962, a large number of concrete blocks with a side length of 1 m were manufactured in cooperation between a number of services and establishments and the temperature generation was measured [lit. 13]. The aim was to investigate which cement and concrete compositions ensured the lowest increase in temperature.
The results showed that even in the most favourable case (blast furnace cement A), the temperature increase was 20°C.

Setting is followed by a gradual fall in temperature as a result of which concrete, which is able to deform freely, will contract in proportion to the fall in temperature. If deformation of the concrete is completely prevented, tensile stresses occur. For a temperature drop of 20°C, these stresses will, if no cracks develop, theoretically amount to about 500 N/cm², i.e. greater than the tensile strength of concrete which is approximately 300 N/cm² for concrete B 225.
The stresses which occur when deformation is prevented also depend on the modulus of elasticity and creep characteristic. The modulus of elasticity (see 3.2.6 and fig. 14) of unhardened concrete (1 to 2 days old) is very low.

SHRINKAGE

Concrete shrinks when water which is not yet bound evaporates through the pores and capillaries. The extent of the shrinkage depends of the composition of the concrete, subsequent processing and the dimensions of the structural element. In the case of massive structures, provided they are properly executed, shrinkage will be less than in thin structures because the capillaries do not form a continuous network; evaporation of water within the concrete is therefore inhibited. For the same reason, massive concrete is waterproof.
In the case of thin structural elements, the shortening due to shrinkage may be of the same order of magnitude as that due to a temperature drop of 20°C. If deformation is prevented, the same consideration applies to tensile stress as in the case of a temperature drop.

CREEP

This term generally denotes deformation of concrete increasing with time, which occurs only as long as the concrete is under stress. Creep is very considerable in the case of concrete which is a few days old (see 3.2.6). The same phenomenon also means, however, that stresses in concrete whose deformation is prevented will decline with the passage of time. Suffice it to say for the time being on this point that if massive concrete reaches the ambient temperature after setting without cracks, the likelihood of an increase in tensile stresses is reduced.

It is apparent from the above that the principal factors influencing the formation of cracks in massive structures are the maximum temperature increases reached during setting and the possibility of deformation.

When tunnels are built the floor is generally poured first. Deformations due to the temperature drop after the setting process can only be inhibited by shearing stresses between the concrete and subsoil or by horizontal pile reactions.

The dimensions of the floors are, however, generally so small that no great pile reactions can be generated unless very heavy forces are needed to displace the pile heads. For these reasons, continuous cracking rarely occurs in floors. The only risk in the case of massive floors lies in excessively rapid cooling of the surface while the temperature in the core of the concrete is still increasing. As a result, the concrete which is becoming warmer will expand causing tensile stresses on the outer surface while, on cooling, shrinkage of the innermost concrete is prevented by the outer layers so that tensile stresses are generated in the core of the concrete.

Once the floor has hardened, the walls and roof are poured. The heat generated close to the construction joint is conducted away to the floor. This is one of the reasons why no cracks occur immediately above the construction joint.

However a few decimetres above the joint, the temperature may rise considerably.

Schleeh, Kawamoto, Carlson and Reading [lit. 14, 15, 16] have calculated or determined experimentally the stress pattern occurring in a wall on which deformation

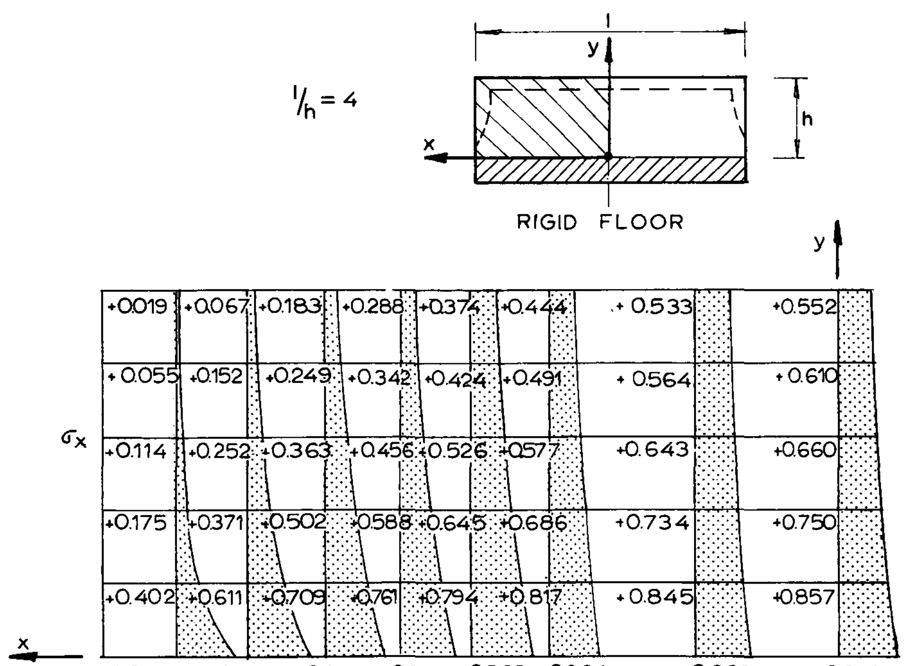

Figure 10. Stresses in the wall.

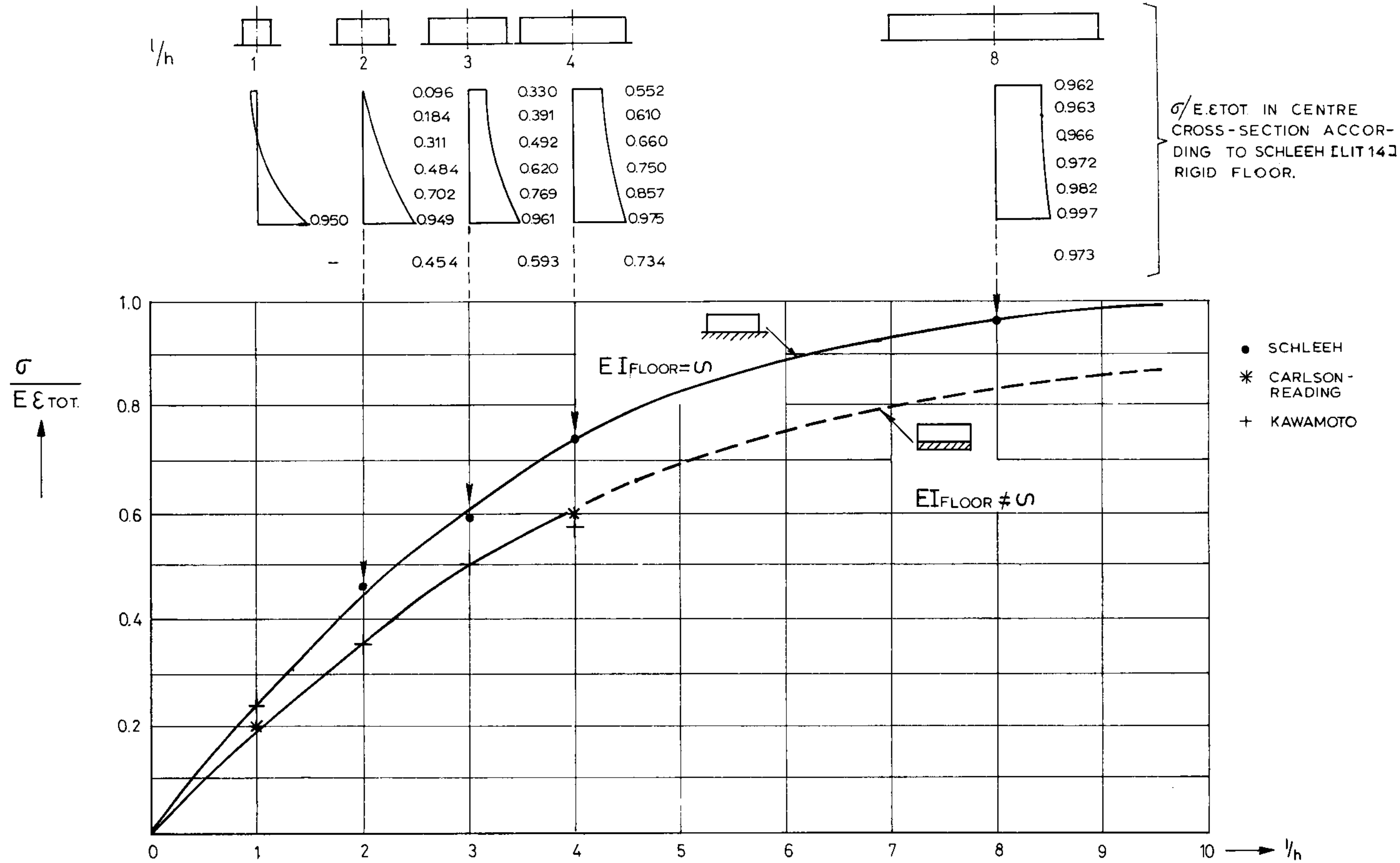

Figure 11. Average stress in cross-section.

of the lower edge has been prevented as a consequence of a temperature drop identical for the entire wall. It is apparent (see fig. 10 and 11) that the stress patterns are dependent on the height to length ratio of the wall. Close to the floor there is an area of stresses which are approximately equal to the stresses occurring if shrinkage is completely inhibited. The height of this area diminishes as the length becomes shorter.
In general, it can be stated that — unless special measures are taken — the concrete of floors will not crack but that in the walls will. The mechanism of crack formation may be summarized as follows with some simplification.
While the temperature in the walls increases (hydratation) deformation is partly prevented by the floor. The modulus of elasticity of the concrete is, however, still so low that only slight compressive stresses can be built up. While the temperature is falling (until it reaches that of the ambient air) the modulus of elasticity is higher and tensile stresses are formed (due to the partial prevention of deformation); these stresses exceed the tensile strength of the concrete, less the compressive stresses built up earlier and cracks occur.

3.2.3 *Prevention of crack formation*

It follows from the above that cracks can be prevented by pouring the walls in narrow sections (with a width of about 5 m); this has been confirmed by practical experience. However, this also means that a large number of vertical joints are formed which must each in turn be made watertight. This is expensive and it is also an expensive proposition to pour the walls in so many different sections.
It also follows from the previous observations that cracks can be prevented by pouring the floor, walls and roof in a single operation so that there are no sections with uneven deformation. For reasons of shuttering techniques, this method can only be applied economically in the case of tunnels with a relatively small cross-section, e.g. the subway tunnel in Rotterdam [lit. 8] or the pipeline tunnels under the Hollandsch Diep and Oude Maas or the Jutphaas conduit [lit. 9].
Longitudinal reinforcement does not prevent crack formation. As long as the concrete has not yet cracked, the stresses in the reinforcing elements are very low. It is only when crack formation begins that high stresses are generated at the location of the cracks. With low reinforcing percentages, the shrinkage forces are so high that the reinforcement yields. The forces thus exerted by the reinforcement are very low and do not influence the crack pattern. With high reinforcing percentages, the reinforcement exerts forces in the cracks on the shrinking concrete so that the cracks occur at shorter distances from each other and the crack width is limited. To limit the crack width, reinforcing percentages of approx. 0.4% per lateral surface are needed. This is expensive for massive structures.
The Amsterdam Public Works Department developed a method in connection with subway construction to prevent crack formation in caisson walls [lit. 18]. According

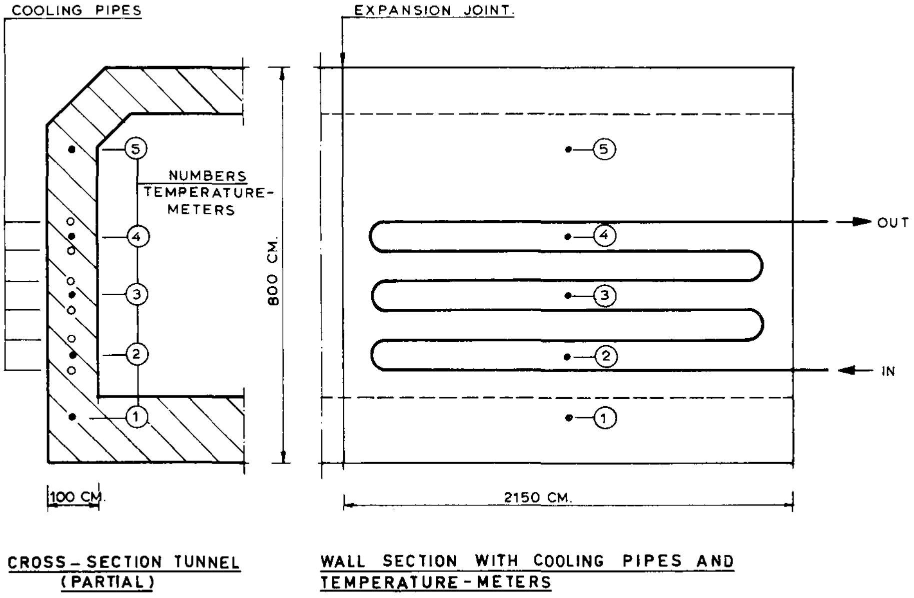

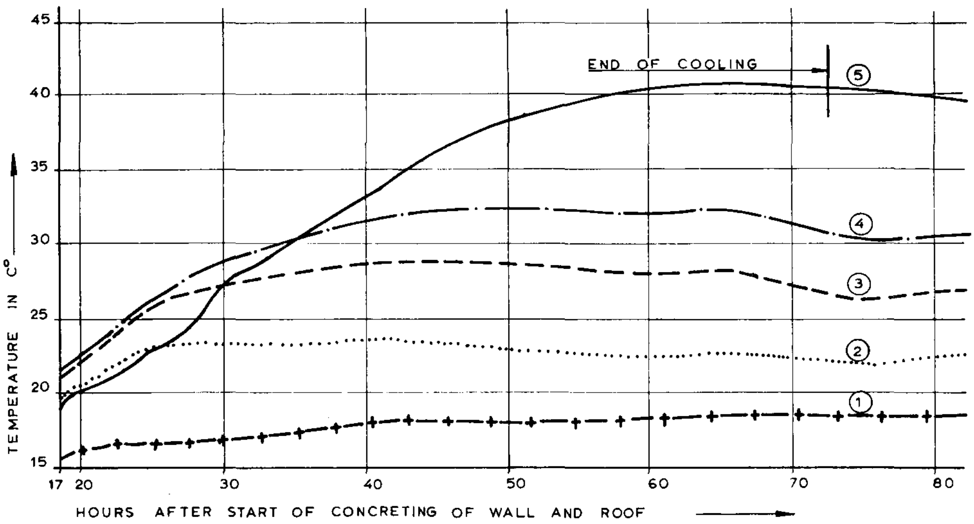

Figure 12. Cooling pipes and temperature development.

to this method, the heat generated during the setting period by the concrete in the walls is conducted away with cooling water. This water is pumped through a tube fitted in a zigzag pattern on the lowest few metres of the walls and placed in position

at the same time as the reinforcing elements before pouring. Figure 12 shows the principle.
Favourable experience with this method led the Vlake tunnel contractor to propose as an alternative solution cooling of the tunnel walls and omission of the waterproof lining.
Cooling and stress calculations combined with laboratory tests showed that this method should also be successful for the Vlake tunnel. In addition, the composition of the concrete was adapted in such a way that the heat generation, water penetration and shrinkage would be limited as far as possible.
Now that the concrete work on the tunnel has been completed, the cooling method has been found to have prevented crack formation here too. Figure 12 shows the results of temperature measurements on a cooled wall.
The method of calculation is discussed in further detail in 3.2.4 and 3.2.5. Attention

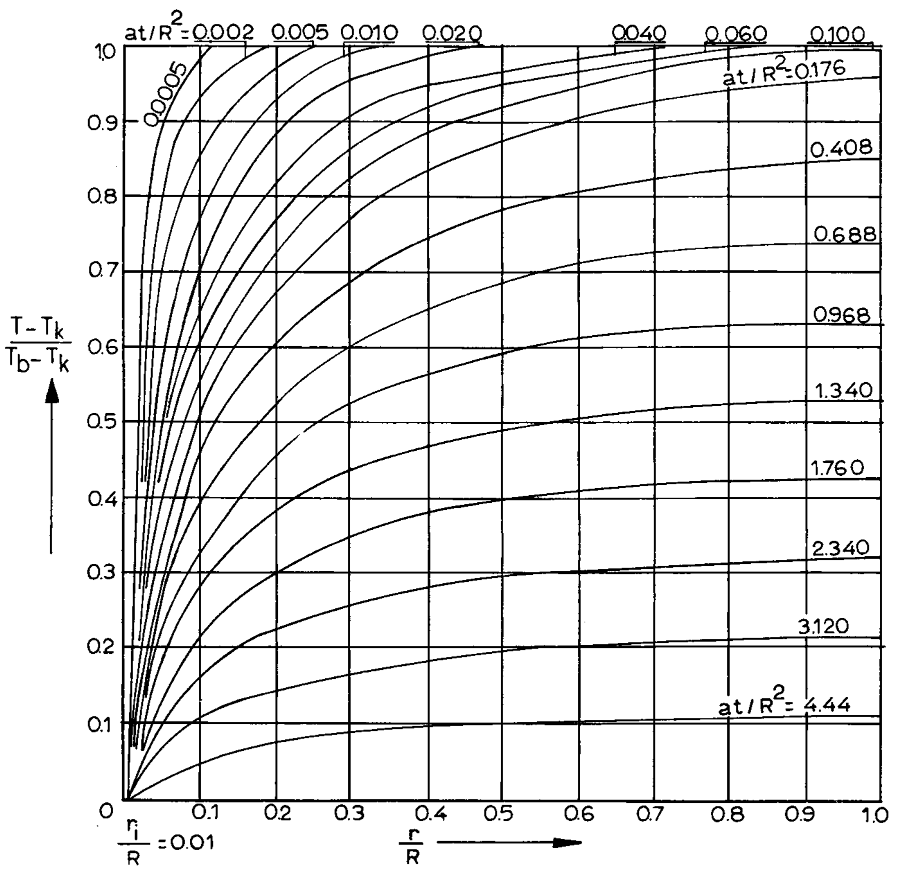

Figure 13. Temperatures in a concrete cylinder around the cooling pipe.

should, however, be drawn already at this stage to one important result of the calculations.

In the case of uncooled walls, the temperature falls very slowly so that the dangerous tensile stresses occur only after a few days.

On the other hand, with cooled walls (according to the calculation) tensile stresses occur already after about two days, especially if the cooling process is continued for too long. These stresses are admittedly much lower than in uncooled walls but they occur at a time when the tensile strength of the concrete is still low. For these reasons a study has been undertaken of the development of the tensile strength of fresh concrete.

3.2.4 *Calculation of cooling*

Mandry [lit. 17] describes how the temperature of a concrete cylinder diminishes as a function of place and time. The basic assumptions in this approach to the problem are as follows:

1 At $t = 0$ the cylinder has a temperature of T_b at all points.

2 No heat is produced and no heat flows away to the environment through the outside walls.

3 The cooling water always has the same temperature T_k.

Figure 13 shows that there is a strong gradient close to the cooling pipe but the temperature characteristic quickly flattens out. As a result the mean temperature is somewhat lower than the maximum temperature. The following expression is obtained for the mean temperature:

$$T = T_k + (T_b - T_k).e^{-\beta t} \tag{5}$$

in which

$$\beta = \frac{a\ (0.7 + 4\frac{r}{R})^2}{R^2}$$

a = coefficient of thermal conductivity of concrete,
r = radius of cooling pipe,
R = radius of concrete cylinder.

The formula is also a solution to the differential equation

$$\frac{dT}{dt} = -\beta\,(T - T_k) \tag{6}$$

In other words, the reduction in temperature is proportional to the difference in temperature between the concrete and cooling water.

In a long cylinder allowance must be made for heating of the cooling water from the point of entry. The mean concrete temperature then becomes a function of the distance (x) from the point of entry and the time (t).
In addition to equation (6) which must now be written with curve d's, we also require a balance equation for the temperature of the cooling water.
This is as follows:

$$\frac{\delta T_k}{\delta t} + U \frac{\delta T_k}{\delta x} = \frac{C_b \gamma_b F_b}{C_w \gamma_w F_w} \beta (T - T_k) \tag{7}$$

C_b, C_w = specific heat of concrete and cooling water,
γ_b, γ_w = specific weight of concrete and cooling water,
F_b, F_w = surface area of cooled zone and cooling pipe,
U = flow velocity of the cooling water.

According to Mandry, the approximate solutions to (6) and (7) are as follows:

$$T_k = T_{k_o} + \frac{\beta}{K+\beta} (T_b - T_{k_o})\, e^{\frac{-K\beta}{K+\beta} t} \tag{8}$$

$$T = T_{k_o} + (T_b - T_{k_o})\, e^{\frac{-K\beta}{K+\beta} t} \tag{9}$$

in which

$$K = \frac{C_w \gamma_w F_w U}{C_b \gamma_b F_b x}.$$

If we write for $\frac{K\beta}{K+\beta} = B$, (9) becomes

$$T = T_{k_o} + (T_b - T_{k_o})\, e^{-Bt} \tag{10}$$

in which
B is a function of x.

It is thus apparent that the temperatures drop at all points according to a power of e, but that the characteristic becomes less marked the greater the distance from the point of entry.
If heat is produced, equation (6) changes to:

$$\frac{\delta T}{\delta t} = \frac{dT_a}{dt} - \beta\,(T - T_k)$$

in which

T_a is the temperature which occurs if there is no cooling, in other words if $\beta = 0$.

The solution then becomes:

$$T = T_{k_o} + (T_b - T_{k_o})\, e^{-Bt} + \int_o^t \frac{dT_a}{dT}\, e^{-B(t-T)}\, dT \qquad (11)$$

Expressed numerically, the integral is:

$$\sum_{n=1}^{i} \Delta T_{a_n}\, e^{-B\,(t-t_n)} \qquad (11a)$$

In other words, any contribution to the increase in temperature of uncooled concrete is reduced by the same power of e.

Formula (11) can therefore be used to determine for any given point the temperature characteristic for different cooling water flow rates and cooling water temperatures, provided that the temperature characteristic in uncooled concrete is known.
In determining the cooling pipe dimensions, the wall is treated as the theoretical concrete cylinder whose surface area is determined by the distances between the cooling pipes and the wall thickness.

3.2.5 *Stress calculations*

The temperatures have now been calculated as a function of height and time. How are the associated stresses to be calculated? Four basic assumptions are used here.

1. The stress-elasticity-temperature-time relationship:

$$\frac{d\sigma}{dt} = E\,\left(\frac{d\varepsilon}{dt} - \alpha\,\frac{dT}{dt}\right) \qquad (12)$$

The stress σ is positive during tension.

ε is positive during contraction,

α is the coefficient of expansion (10^{-5}/°C),

E is the modulus of elasticity which is a function of time

t. However, E is constant in the case of the floor,
T is the temperature.

2. The deformation characteristics are a linear function of the height y (plane-sections remain plane):

$$\varepsilon = \varepsilon_o + \frac{\varepsilon_b - \varepsilon_o}{h} y \tag{13}$$

ε_o is the contraction of the lowest fibre and ε_b that of the highest;
h is the total height.

This assumption does not apply close to the ends.
This assumption also supposes that the tunnel segment as a whole can adopt a curvature and change its length.

3. In each cross-section the resultant horizontal force is zero. No allowance is made for the influence of shearing forces or pile reactions along the lower surface of the tunnel floor.

4. In each cross-section the resultant moment is zero. It is thus assumed that the curvatures are sufficiently small for no important changes to be brought about in the bearing reactions. This clearly only applies to sections of limited length (the tunnel, i.e. both the approaches and the immersed section, is generally cast in section lengths of approx. 20 m, expansion joints being fitted between the sections).

The structure of the calculation is such that the stress changes are determined and added up at successive points in time. During a given time, the modulus of elasticity is considered to be constant so that the stress change in that period is:

$$\Delta\sigma = E\,(\Delta\varepsilon - \alpha\Delta T) \tag{12a}$$

ΔT is positive if the temperature increases.

The expression for the change in length under tensile stress as a function of height, i.e.

$$\Delta\varepsilon = \Delta\varepsilon_o + \frac{\Delta\varepsilon_b - \Delta\varepsilon_o}{h} y \tag{13a}$$

can be substituted here giving the following relationship:

$$\Delta\sigma = E\left(\Delta\varepsilon_o + \frac{\Delta\varepsilon_b - \Delta\varepsilon_o}{h} y - \alpha\Delta T\right) \tag{12b}$$

The third basic assumption (in which b is the width) is:

$$\int \Delta\sigma b\,dy = 0 \tag{14}$$

which, with the expression for $\Delta\sigma$ according to (12b), becomes:

$$\int E\,(\Delta\varepsilon_o + \frac{\Delta\varepsilon_b - \Delta\varepsilon_o}{h}\,y - \alpha\Delta T)\,bdy = 0 \tag{14a}$$

The fourth basic assumption is:

$$\int \Delta\sigma bydy = 0 \tag{15}$$

which in the same way becomes:

$$\int E\,(\Delta\varepsilon_o + \frac{\Delta\varepsilon_b - \Delta\varepsilon_o}{h}\,y - \alpha\Delta T)\,bydy = 0 \tag{15a}$$

With (14a) and (15a) we have two equations for $\Delta\varepsilon_o$ and $\Delta\varepsilon_b$, which can be solved; the stress changes for each height y are then determined with (12b).
When this method is used, a weighted centre of gravity is determined at a distance z from the lowest fibre according to:

$$z = \frac{\int Eybdy}{\int E\,bdy} \tag{16}$$

The origin of the y axis is chosen at this centre of gravity. The equation for changes in length under tensile stress as a function of height becomes:

$$\Delta\varepsilon = \Delta\varepsilon_z + \frac{\Delta\varepsilon_b - \Delta\varepsilon_o}{h}\,y \tag{13b}$$

and the equation for stress changes:

$$\Delta\sigma = E\,(\Delta\varepsilon_z + \frac{\Delta\varepsilon_b - \Delta\varepsilon_o}{h}\,y - \alpha\Delta T) \tag{12c}$$

If y is chosen in relation to the weighted centre of gravity then:

$$\int Eybdy = 0 \tag{17a}$$

By definition the weighted surface area A' is determined by:

$$E_o A' = \int Ebdy \tag{17b}$$

and the weighted moment of inertia I' by:

$$E_0 I' = \int \bar{E} b y^2 dy \tag{17c}$$

Here E_0 is the modulus of elasticity of the hardened floor.
By substituting (12c) in (14) and (15) the following equations are obtained with the aid of 17a, b, c:

$$\Delta\varepsilon_z E_0 A' = \int E\alpha\Delta T b dy = N' \tag{18a}$$

$$\frac{\Delta\varepsilon_b - \Delta\varepsilon_o}{h} E_0 I' = \int E\alpha\Delta T b y dy = M' \tag{18b}$$

With the aid of (13b) it follows that:

$$\Delta\varepsilon_b = \frac{N'}{E_0 A'} + \frac{M'(h-z)}{E_0 I'} \tag{19a}$$

$$\Delta\varepsilon_o = \frac{N'}{E_0 A'} - \frac{M' z}{E_0 I'} \tag{19b}$$

N' and M' are the normal force and the moment which would occur, due to an increase in temperature ΔT, if no deformation of the tunnel section were possible.

Substitution of (18a) and (18b) in (12c) finally gives:

$$\Delta\sigma = \frac{E}{E_0}\left\{\frac{N'}{A'} + \frac{M'}{I'} y - E_0 \alpha \Delta T\right\} \tag{20}$$

in which y is measured from the weighted centre of gravity.

Summarized briefly, the procedure for the stress calculations is as follows:

1 Use equation (11) given in section 3.2.4 to determine the temperatures at different heights and times.

2 Determine the temperature differences ΔT for successive periods of time (positive if the temperature rises).

3 Determine, for each period of time, the weighted centre of gravity, allowing for the fact that E is smaller than E_0 in fresh concrete.

4 Use (17b) and (17c) to determine the weighted surface area and moment of inertia.

5 Use (18a) and (18b) to determine N' and M' after which $\Delta\sigma$ is determined for each point in time with (20).

6 The resultant stress is obtained by adding together the $\Delta\sigma$ values for the previous points in time.

3.2.6 *Concrete tests*

The TNO-IBBC conducted a large number of tests at the request of the Rijkswaterstaat to determine variations in the coefficient of expansion, modulus of elasticity, tensile strength and pressure strength. The tests were conducted in two series, one under cold and the other under warm conditions.
In the cold series the concrete was held at a constant temperature of 11°C from the time of pouring, thus giving an idea of the development of the characteristics of cooled concrete (see fig. 14).

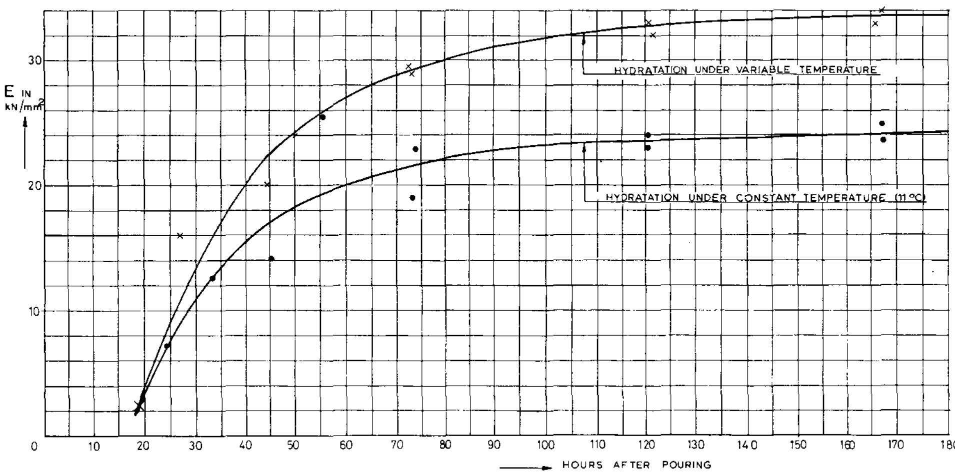

Figure 14. Modulus of elasticity as a function of time.

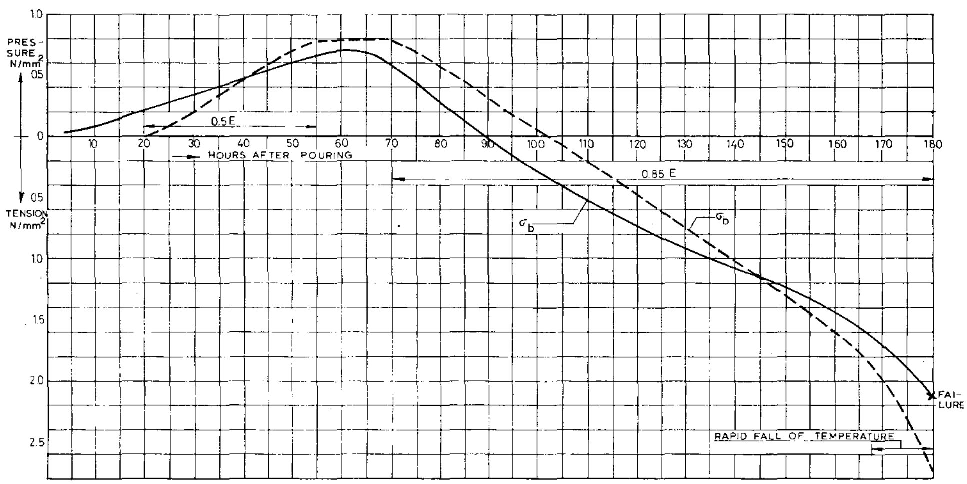

Figure 15. Stresses in a concrete prism hydrating under variable temperature.

In the warm series, the temperature of the concrete was first raised and then lowered according to the temperature pattern measured on cubes of hardening concrete (with a side length of 1 m). This gave an idea of the trend in the characteristics of massive uncooled concrete (see fig. 14).
A concrete prism was also exposed to the above temperature pattern, deformations being prevented (fig. 15). From the forces necessary to prevent deformation it was possible to verify whether the basic assumptions for the stress calculation were correct. The influence of creep was found to be considerable and the theory and measurements could only be reconciled by reducing the measured modulus of elasticity as indicated in fig. 15 by 0.5E and 0.85E. The dotted line represents the results of stress calculations using the reductions, the solid line represents the evolution of the measured stresses.

3.2.7 *Composition of concrete*

For the composition of the concrete a minimum cement content of 275 kg per m^3 is assumed in order to limit the development of heat as far as possible. A lower content is not acceptable, for one reason because of the need to protect the reinforcing elements against corrosion. To ensure adequate strength and waterproof concrete, the content of fine particles (particles smaller than 0.3 mm) consisting of cement, sand and air bubbles must be approx. 160 l per m^3, and the air percentage must not exceed 4%. To keep the water cement factor as low as possible, a plasticizer is added.

3.2.8 *Conclusion*

The cooling method developed for the subway caissons in Amsterdam has now also given good results in a motorway tunnel. The cost of this construction method is lower than the traditional system with a waterproof lining. It seems that the method will be used frequently in the future.
It will, however, be necessary to keep the tunnels built in this way under observation before more general application can be possible. Reliable data has still to be obtained on the behaviour as a function of time (tensile stresses caused by changes in the temperature of the ambient air in the operational stage must be superimposed on the tensile stresses caused by the hydratation process; on the other hand the tensile strength in the operational state is higher than in the initial phase). At the time of writing, the Vlake tunnel has been completed but no experience is available over an extended period.

Finally, the need to implement the method with appropriate care must be stressed. The cooling calculations and control of the cooling system (duration and water temperature) etc. are particularly important. Here it should be noted that cooling must continue for about 10 hours after the topmost cooled concrete has reached its maximum temperature and that the cooling water must be introduced at the bottom of the wall (figure 12) to leave the structure at the top of the wall. In this way the temperature increases from the bottom upwards and the cooling effect at the top is reduced so that a gradual increase in the concrete temperature is obtained from the bottom upwards (fig. 12), i.e. from the concrete floor which has already hardened through the cooled, setting concrete in the walls to the uncooled setting concrete in the roof. If these criteria are not complied with, local temperature surges may cause cracking.

3.3 Hydrodynamic study

3.3.1 *Introduction*

If a tunnel under a river is built by the immersed tube method, the tunnel elements will be exposed to flow forces during the immersion operation. These forces are due to the fact that the tunnel element prevents the undisturbed flow of part of the water. The water which originally flowed through the area blocked by the tunnel element is now deflected at higher flow velocities through an area around the tunnel element.
These local increases in current speed around the tunnel element are due to the fact that a pressure drop is established over the tunnel element which also implies the generation of a flow force on the element. If the extent of the area in which the flow rate is accelerated around the tunnel element is limited by the presence of a fixed obstacle such as a river bed or bank, the flow speeds in the area of acceleration must increase additionally to discharge the blocked part of the river flow through the reduced cross-section. This will be effected at the cost of an additional drop over and flow pressure on the tunnel element. Clearly the greater the rate of blockage of the flow profile of the river, the greater the drag force on the tunnel element will be.
The forces acting on an object in flowing water have a dynamic character and may be divided into a mean force and a force fluctuation. During the immersion operation, the tunnel element is clamped into a cable system with carefully calculated cable rigidities. The dynamic flow forces thus act on a mass-spring system and generally lead to erratic but not extreme oscillating movements. In some particular cases (if the damping is low enough) heavy oscillating movements of the tunnel element and considerable fluctuations in the cable forces may be caused by phenomena of resonance if the frequency of the fluctuations in the flow force approaches a resonance frequency of the mass-spring system.

In order to determine the dimensions of the cable system used to immerse the tunnel elements and to define the conditions under which immersion can still take place satisfactorily, it is necessary to predict fairly accurately the drag forces acting on the tunnel elements and the movement of those elements as a result of different flow conditions. One highly satisfactory method of doing this is to carry out a model test in a hydraulics laboratory.

3.3.2 *Models with identical hydraulic and dynamic characteristics*

In a hydraulic model the geometry of the prototype is reproduced on a smaller scale so that it is possible relatively easily and quickly to study a prototype situation or a number of alternative situations.
The conditions to be met by a hydraulic model are that all the terms in the equation of motion relevant to the study are uniformly reduced in size. These conditions lead to a number of scale rules or model laws, Froude's and Reynolds' scale rules being the best known.

If a complete picture is required of the forces acting on a tunnel element and the movement of that element, the study must be carried out in a model which is dynamically equivalent to the prototype. All the forces acting on the tunnel element must be reproduced true to scale, in particular:
— flow forces on the tunnel element (pressure and friction);
— mass — inertia forces;
— cable forces;
— damping forces in the event of oscillations.

By giving the model the same geometrical shape as the prototype and basing it on Froude's scale rule (velocity scale = root of height scale) the flow forces and mass inertia forces will be reproduced accurately in the model if the flow is sufficiently turbulent (Reynolds' number). The reaction forces in the vertical cables between the tunnel element and the pontoons from which the element is suspended during immersion (see also fig. 6) are proportional to the draught increase of the pontoons. Because of the geometrical similarity, the force-movement relationships for the vertical cables are also accurately reproduced in the model.
During the immersion manoeuvre, the tunnel element is anchored to six horizontal cables: 2 in the axis of the element (one in front and one behind, made fast to the outer ends of the element) and 4 approximately perpendioulairly to its axis, secured to the outer corners. The attachment points required for this purpose are provided on top of the element.
The reaction forces in these cables are generated by tensile stress on the cables when the tunnel element is moved. Based on an accurate reproduction (true to scale) of the horizontal force — movement relationships, substitute elastic rigidities can be determined in the models for the cables so that the clamped tunnel element is correctly reproduced in the model as a mass-spring system.

The hydraulic damping forces due to the mass inertia of water are reproduced well in a model based on Froude's scale rule. The dynamic character of the force pattern in the horizontal cables in the model may, however, deviate from the true situation. The reason for this is that it is partically impossible to ensure that the model cables comply both with the elasticity requirement and with the geometrical condition. As a result, the damping effect of the own weight of the cables on the force pattern in the cables (weakening impacts) is not correctly reproduced in the model. This departure from the real situation may under some circumstances influence the reliability of the dynamic part of the study (fluctuations).

3.3.3 *Model study for the Drecht tunnel*

As an example of a hydraulic model study, the study of the Drecht tunnel is discussed in more detail in this section.
This tunnel is being built under the Oude Maas between Zwijndrecht and Dordrecht and is to replace the existing bridge on national highway 16 which is too narrow (fig. 16).

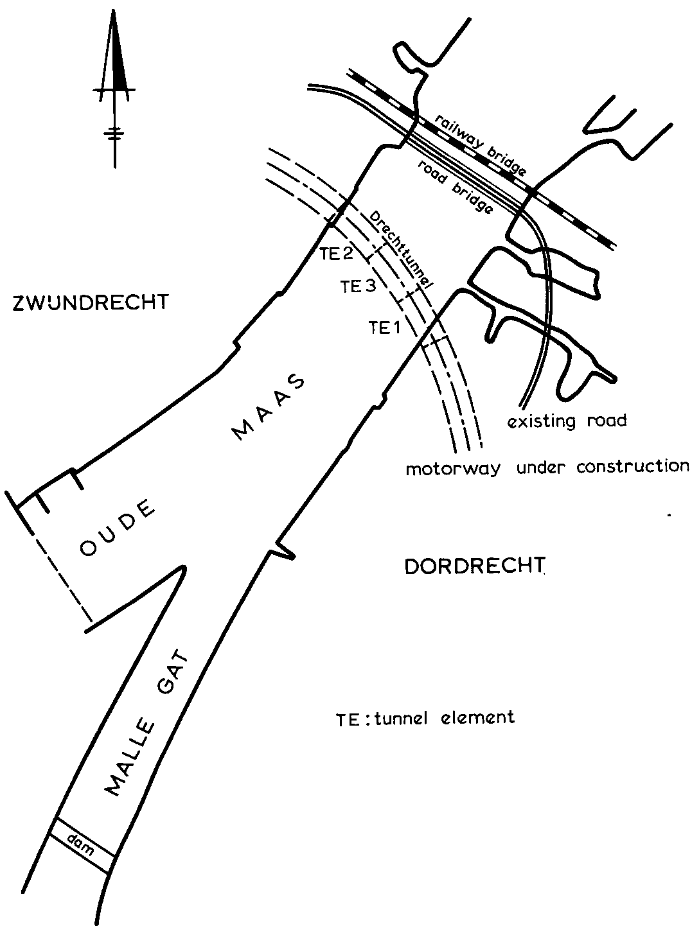

Figure 16. Site plan Drecht tunnel.

The construction of the land section of the tunnel with 8 traffic lanes and a total length of 825 m is described in section 3.1.
The section of the tunnel to be immersed consists of 3 tunnel elements, each with a length of approx. 115 m and a width of 49.04 m. All the elements are bent in the horizontal plane (R = 800 m). Viewed in the vertical plane, the central element is bent at a constant radius (R = 2,500 m) over its entire length and the two elements on either side are partially bent and partially straight. The height of the central element varies between 8.08 and 8.57 m and the value is constant for the two others (8.08 m).
The tunnel elements are to be built in an existing dock near Barendrecht. On completion they will be towed floating on the Oude Maas to Dordrecht over a distance of about 12 km. Because of the great depth of the floating tunnel elements, the navigation channel of the Oude Maas will have to be locally deepened to allow transport between the construction dock and the immersion trench at Dordrecht. Because the transport of such a large object, which is also curved in two directions, through a relatively narrow river is a unique operation, no sufficiently accurate estimate could be given of the likely drag forces on the basis of existing knowledge. The Rijkswaterstaat therefore entrusted the Delft Hydraulics Laboratory with the task of studying the extent of the drag force on the tunnel elements and their dynamic behaviour during transport. This study is described in more detail in section 3.3.4.

After the tunnel elements have been towed into position by tugs, they will be clamped into a cable system at the site of the immersion trench and thus brought to the exact location and immersed; the elements 2, 1 and 3 will be dealt with in succession (see fig. 16). To determine the dimensions of the cable system and the conditions under which immersion can still be effected satisfactorily, it is desirable to have the most accurate possible knowledge of the forces acting on the tunnel elements and their movements in the different immersion phases. For this reason, a study was also carried out by the Delft Hydraulics Laboratory for the immersion phases. It is described in section 3.3.5.

3.3.4 *Transport from the construction dock to the immersion trench*

The study was carried out in a model based on Froude's scale rule with a length scale of 1:50. As data only had to be acquired for the most unfavourable situation, a simplified model was sufficient. A river section with a length of 1 km was reproduced in the form of a linear prismatic channel with a schematized cross-section. This cross-section was based on the decisive cross-section of the Oude Maas with a groin on both sides. The study is simplified by not towing the tunnel element but adjusting the relative speed of the tunnel element and the water solely through the flow velocity of the water. The tunnel element is held in place by a cable system during the measurements.

The tunnel element is reproduced geometrically true to scale in the model and was also ballasted in such a way that the mass inertia moments were properly reproduced.

The study was carried out at an early stage in conjunction with the design and construction of the tunnel elements for the Drecht tunnel. The mean depth of the floating tunnel element was taken as 7.50 m (this later became 7.65 m for elements 1 and 2 and 8.08 m for element 3) and the bed of the navigation channel in the Oude Maas was fixed at a minimum of N.A.P. (Normal Amsterdam Level) — 9.00 m (which later became N.A.P. — 9.70 m on the basis of more recent soundings).

To determine the transport plans for the three tunnel elements, it is necessary to know the required tow forces for different tow speeds in relation to the flowing water. With a known tow capacity, the feasible relative tow speed can thus be fixed. This speed and the known current velocity in the Oude Maas then determines the absolute speed of the tug and towed tunnel element. The tow force is determined by a number of factors the most important being:
a — the relative towing speed;
b — the blocking factor: area exposed to flow/area of river cross-section (A/F);
c — ratio of draught of tunnel element to water depth (d/D);
d — shape of tunnel element and
e — position of tunnel element in relation to river axis (current velocity profile).

The shape of the tunnel elements was a fixed parameter; the flow velocities were varied from $v = 0$ m/s to $v = 1.50$ m/s in stages of 0.30 m/s and the water depth in stages of 0.50 m from $D = 8.50$ m to $D = 10$ m. It must be noted that the Oude Maas is a tidal river in which both the water levels and current speeds vary.
Because of the changes in water depth, the parameters d/D and A/F are in fact also changed. The influence of the parameter A/F was investigated at constant values for d/D by placing the tunnel element at an angle of $+15°$ and $-15°$ to the river axis. This oblique positioning was effected towards both sides in view of the bent shape of the tunnel element. The tunnel element was then investigated in five different positions: situated between 25 m right and 25 m left of the river axis in stages of 12.5 m.
All these tests were designed to determine the forces on the tunnel element. They were carried out on a tunnel element held in place by wires with three force meters.

The drag forces vary as a square function of speed so that they can be expressed by:

$$K = C_d \cdot \tfrac{1}{2} \varrho A v^2 \qquad (21)$$

in which
K = drag force (N),
C_d = drag coefficient (—),
ϱ = density of water (kg/m^3),

A = tunnel surface projected onto a plane perpendicular to the direction of flow (m^2),

v = flow velocity in the unblocked river cross-section relative to the tunnel element (m/s).

Using this equation the drag force can be determined in a given situation with known current velocity if the drag coefficient which depends primarily on the geometry is known. The following table shows the drag coefficients known from the measured forces in the flow direction on the tunnel element in the axis of the river without oblique displacement in relation to the river axis ($\alpha = 0°$).

Table 3

D m	A/F —	$\bar{d}/D$ —	$\bar{C}_d$ —	ΔC_d —
8.50	0.360	0.883	2.9	±0.5
9.00	0.335	0.834	2.45	±0.25
9.50	0.314	0.790	2.2	±0.13
10.00	0.395	0.750	1.9	±0.10

It must be noted that there was a clear tendency for the drag coefficient to increase to some extent with rising current velocity. This increase was all the more marked the lower the water depth and the higher the values for $\bar{d}/D$ and A/F. For the flow velocity range investigated, the deviations are shown in the last column of table 3. This phenomenon can be explained because the parameter $\bar{d}/D$ is not in reality constant but increases through immersion of the tunnel element as the current speed rises (fig. 17).
The partial sinking of the tunnel element is mainly caused by the return current effect which results from the practically identical sinking of both ends of the tunnel elements (fig. 17).

As regards the forces in the direction of flow, there does not appear to be any (significant) difference depending on whether the tunnel element is in the axis of the river or not. This applies at least to deviations of up to 25 m from the axis. There is also no (significant) difference if the tunnel element can move freely in the transverse direction. On the other hand oblique positioning of the tunnel element in the river (photo 7) has, as might be expected, a considerable influence on the force in the flow direction as a consequence of the increase in A/F. As a result the drag coefficient and the secondary influence due to a drop in the water level (further sinking through stronger return current) increase substantially (see fig. 18). This increase is greatest when the concave side of the tunnel element is upstream. This is due to stronger

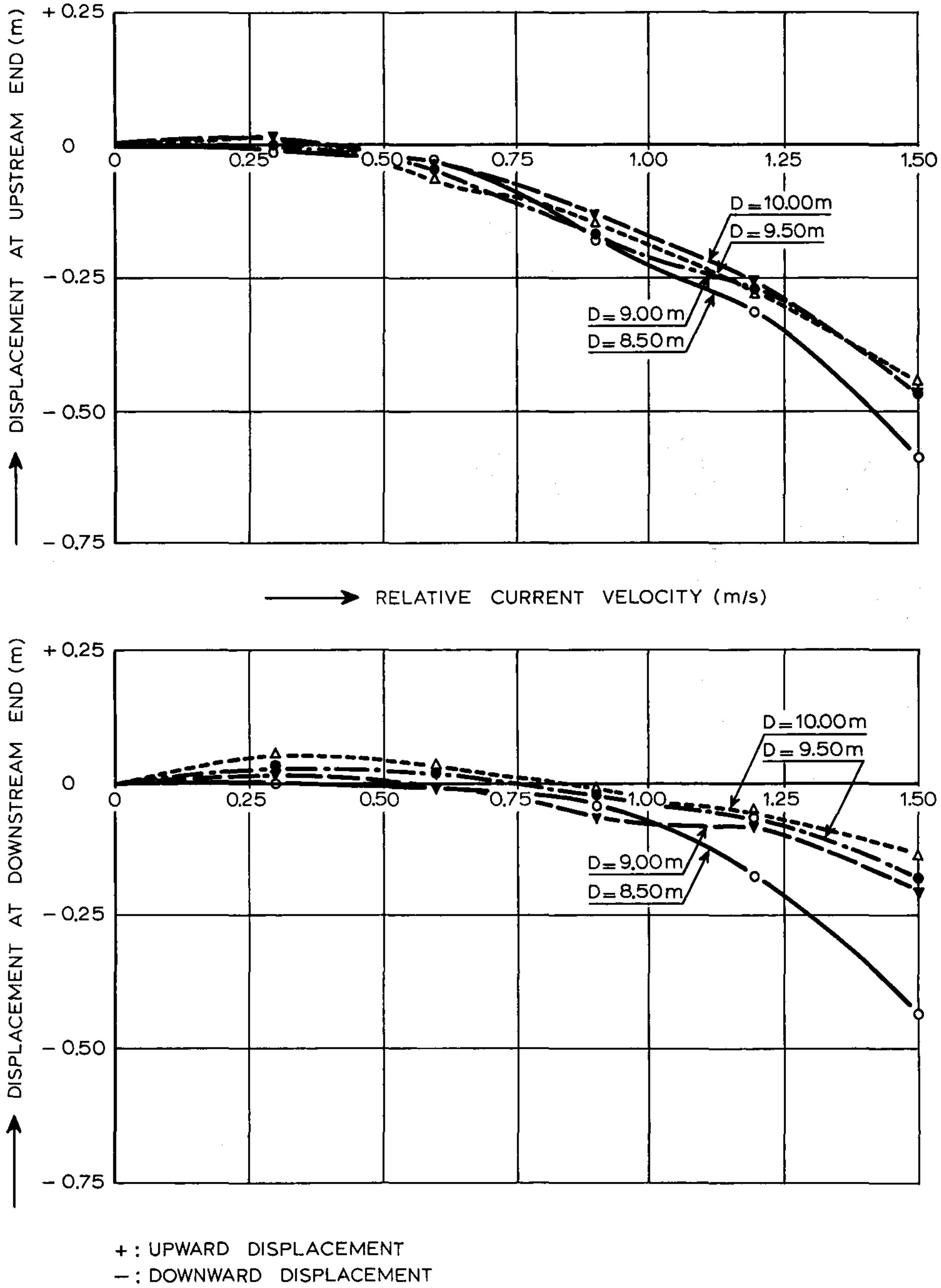

Figure 17. Vertical displacements of tunnel element during transport.

contraction (the current tends to be directed towards the bank). In the case of oblique positioning there also proves to be a considerable force on the tunnel element perpendicular to the flow direction (rope ferry effect). This force represents approximately 35 to 45% of the force in the direction of flow at an angle $\alpha = 15°$.

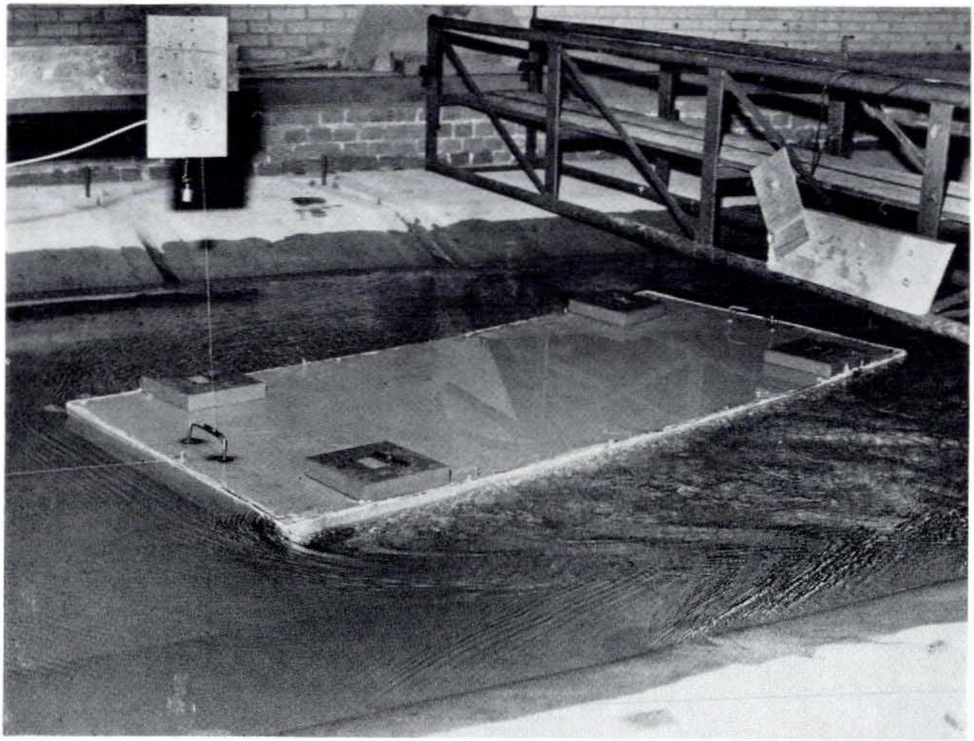

Photo 7. Drecht tunnel; model test for floating transport of the tunnel elements.

The dynamic behaviour of the tunnel element was investigated by securing the element only to the upstream head wire, thus allowing movement at right angles to the flow direction. These tests showed that the tunnel element tended to oscillate around a situation of equilibrium and, at least in the linear prismatic river section in the model, tended to seek the centre of the river. In general, the maximum amplitude of oscillation occurred at the downstream end of the element and did not amount to more than 10 m. Only once was a deviation of 20 m observed for a situation with $D = 8.50$ m and $v = 1.50$ m/s; there is a tendency for the amplitude to reduce as the drag coefficient deminishes. The fact that the element remains in stable oscillation during the situation considered here can be explained by the fact that if the tunnel element deviates in relation to the point of suspension, the movement of the upstream side is inhibited by the fact that the draw cable moves at an angle to the flow direction.

The tunnel element then slews round, creating a force perpendicular to the direction of flow; this is higher the more the downstream side deviates from the situation of equilibrium. This force thus has a strong damping effect on the oscillations and pulls the tunnel element back to the state of equilibrium.

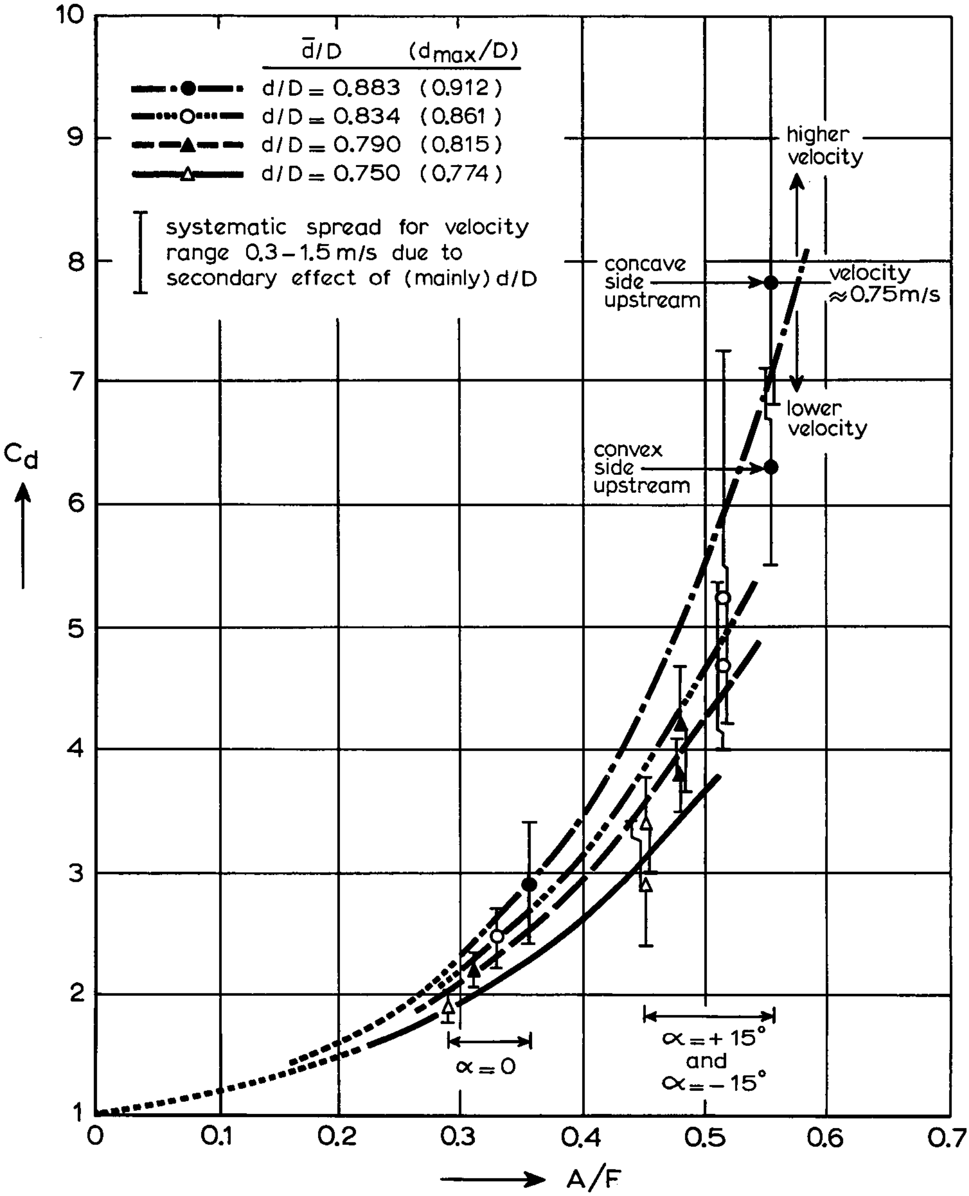

Figure 18. Drag coefficient C_d for transport of elements.

Finally a number of tests were carried out to determine the added mass of the tunnel element. This is the mass of water in the immediate vicinity of the tunnel element which, when the element is accelerated or retarded, is also accelerated or retarded. To help in determining the manoeuvrability of the convoy it is desirable to know this extra mass or the total mass to be accelerated or retarded (virtual mass). This is ascertained by accelerating the tunnel element with a known force and measuring both the force and the velocity characteristics. With the aid of the known force and the calculated acceleration at time $t = 0$, the virtual and added mass can be determined by Newton's law ($K = m.a.$). The test result showed that an added mass corresponding to approx. 10% of the mass of the tunnel element must be expected.

3.3.5 *Immersing the tunnel elements*

The principal data for the immersion phases in which the elements are clamped in the cable system were determined in a hydraulic model with identical dynamic characteristics on a scale of 1/50 (see section 3.3.2). In this model, based on Froude's scale rule, a river section with a length of about 2.1 km was reproduced under accurate geometrical conditions with the immersion trench for the tunnel located in the centre (fig. 19).

The investigated tunnel elements 1 (to be immersed second) and 3 (to be immersed last) were also built to scale according to the specification drawings as were the pontoons from which the elements were suspended during immersion. The changes in flow as a result of the local tidal influence were sufficiently slow to make the inertia effect on the current distribution negligible in relation to the forces on the tunnel elements. It is therefore unnecessary to simulate the tidal movement in the model and the problem can be investigated under permanent flow conditions.

Before carrying out the actual investigation, the current-velocity distribution in the model was calibrated. For this purpose, the flow was arranged in the model with the river bed situation without the navigation channel and the immersion trench for the tunnel elements, in such a way that the flow-velocity distribution in the model coincided well with a distribution measured in the field.

Following the phase of calibrating the model, the immersion phases IV-VII of tunnel elements 1 and 3 (fig. 20) were examined for different flow conditions. Phases VI and VII are the actual immersion phases in which:
—VIa = whole tunnel element just under water,
—VIb = top of tunnel element 2.75 to 3 m (centre) under water,
—VIc = top of tunnel element approximately 4.5 m (centre) under water,
—VII = top of tunnel element 1 approx. 4.5 m (centre) under water and tunnel element 3 approx. 8 m (centre) under water.

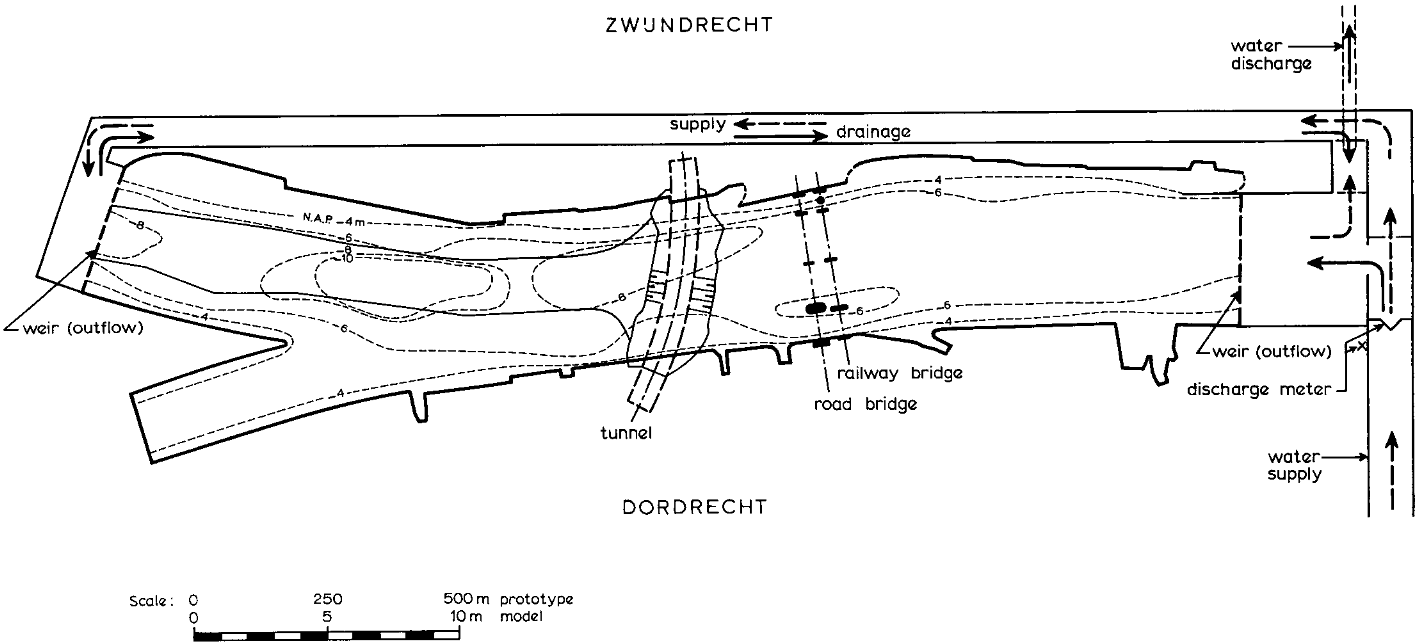

Figure 19. Model layout.

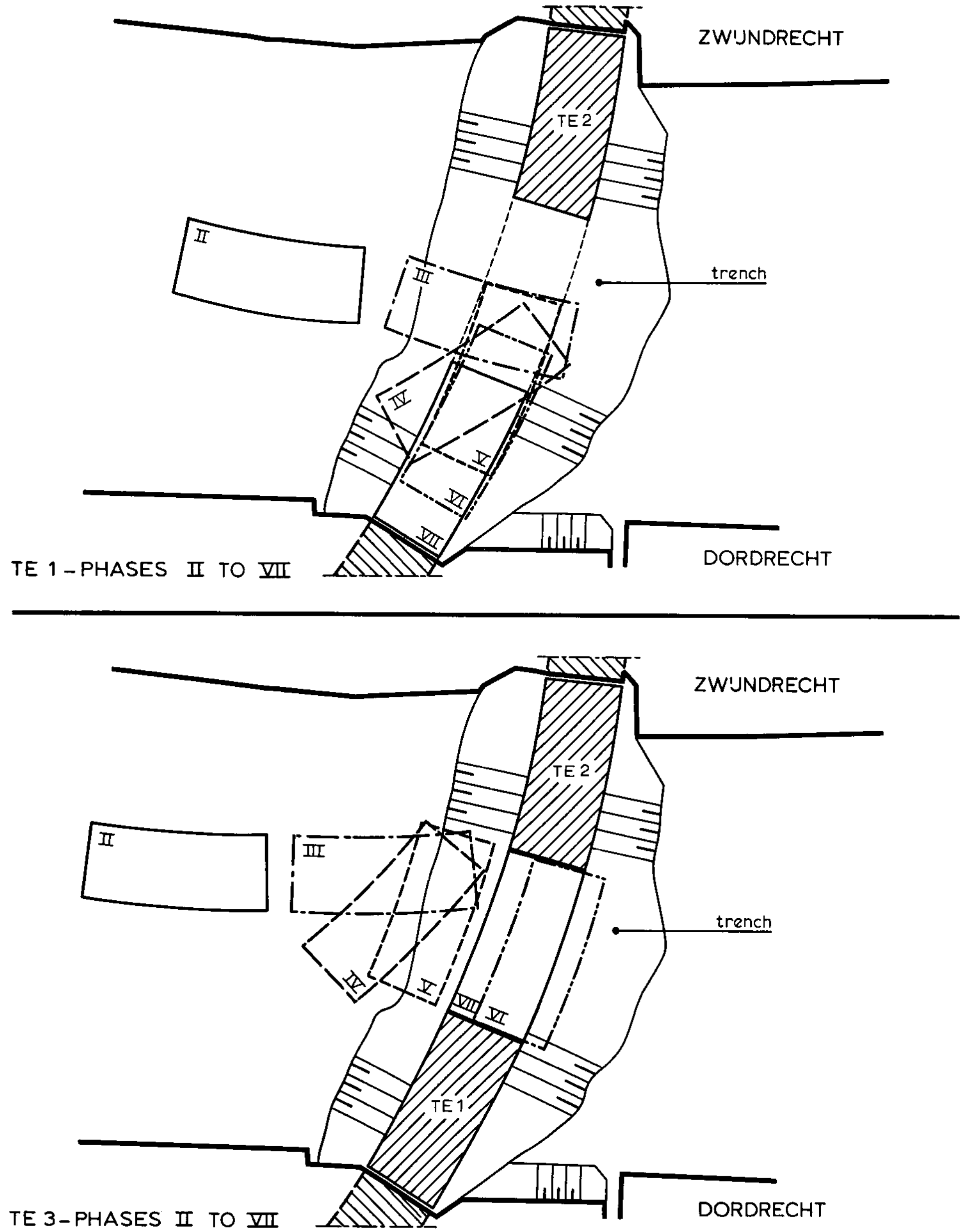

Figure 20. Final phases of positioning elements 1 and 3.

The remaining phases were carried out with a floating tunnel element with a clearance above water of approx. 0.25 m in the centre, i.e. a draught of 7.84 (element 1) and 8.32 (element 3). Both elements were studied for 3 water levels, i.e. —0.50 m, + 0.25 m and + 1.00 m respectively in relation to N.A.P. At each water level the flow rate of the Oude Maas was varied, i.e. 500 m^3/s, 1,000 m^3/s, 1,500 m^3/s and 2,000 m^3/s respectively in the ebb direction (decisive). The highest flow coincides with a discharge of 6,000 m^3/s from the upper Rhine.

During the study, the tunnel elements were clamped in a cable system with corresponding anchor points coinciding with the design plans of the consortium of contractors building the tunnel. The cable system in the model was adapted in such a way that the horizontal flow forces could be measured in three of the six horizontal cables, while the substitute cable rigidities in the model were such that the force-displacement ratio was reproduced true to scale. This is an essential condition if possible force fluctuations on the prototype are to be measured in the model.

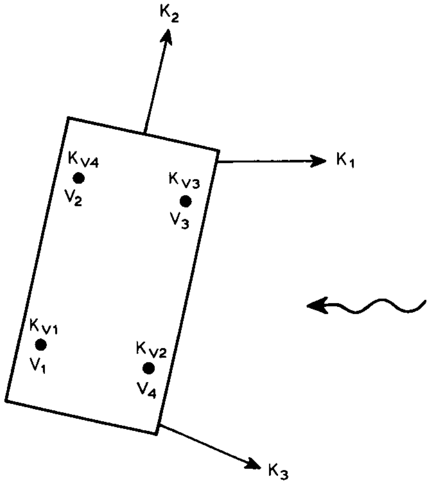

Figure 21. Measuring locations.

The mean values of the measured horizontal cable forces K_1, K_2 and K_3 (fig. 21) varied in all the situations in a square relationship to the river flow so that in the immersion phase equation (21) from section 3.3.4 can also be used for the description of the total mean horizontal drag force. As an example, fig. 22 shows the forces measured in one of the cables (K 1) observed in phase IV for the tunnel element 3. For all the situations studied, equation (21) is used to calculate for the total mean drag forces, the Cd values, the current velocity being defined as the mean current velocity in a calibrated section of the river without a deepened navigation channel (transport of elements) and without the immersion trench:

$$v = Q_{O.M.}/(1870 + 275\ h) \qquad (22)$$

in which

$Q_{O.M.}$ = flow through Oude Maas (m^3/s),
1870 = surface below N.A.P. for calibrated section (m^2),
275 = width of river at N.A.P. for calibrated section (m),
h = water level in relation to N.A.P. (m).

This definition of v discounts the influence of profile changes in the river (due to the immersion trench and the locally deepened navigation channel for the tunnel elements) on the values found for the drag coefficient. So these values apply only to the situations studied and to the defined, decisive current velocity.
The drag coefficients determined from the model results are shown in fig. 23, the characteristic being outlined as a function of the immersion phase. Clearly, the decisive situation for the cable system is determined by phase IV-V for tunnel element 3. In this phase the tunnel element is still slewed in the river perpendicular to the current above the relatively shallow bed of the navigation channel giving a blocking factor $A/F = 0.45$ to 0.55 for the water level at N.A.P.—0.50 m. In conjunction with a flow concentration through the opening between elements 1 and 2 which have already been immersed, this results in the high flow force observed. This force diminishes during this phase through the higher water level (reduction in A/F and d/D). The flow force also falls off substantially because of the considerable widening of the profile

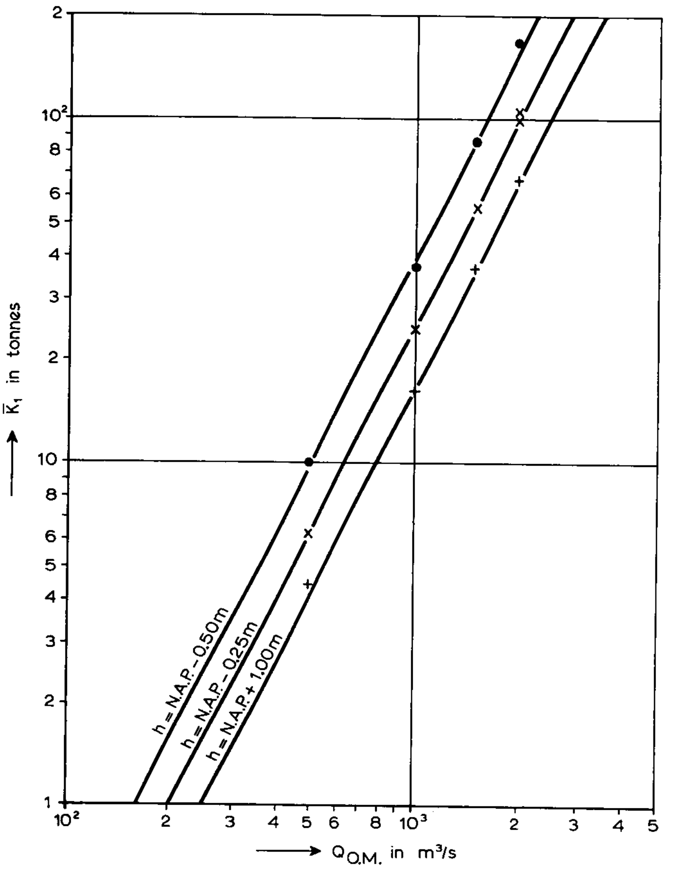

Figure 22. An example of the model results: mean horizontal cable forces.

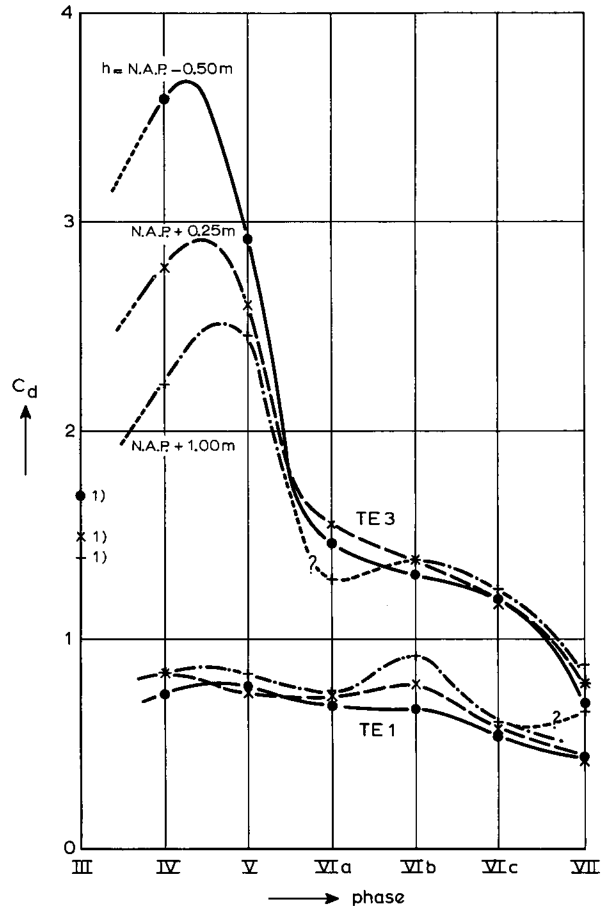

$K = \frac{1}{2}\rho C_d A v^2$ with $v = Q_{Q.M.}/(1870 + 275h)$

1): derived from fig.18

Figure 23. Drag coefficient C_d during positioning of elements 1 and 3.

at the location of the immersion trench (sharp reduction in A/F and d/D), while the immersion of the element in the trench leads to a further fall in the drag force as soon as the element drops into the trench and leaves the main current of the river (phases VIc and VII in comparison with phase VIb).

In regard to the dynamic characteristics, namely force fluctuations, the model was found not to be reliable because of interfering factors on the inflowing water (boundary effects in a model). The small interfering waves (height 0.5 to 1 mm) caused by the inflowing water had a frequency which corresponded approximately to the resonance frequency of the clamped tunnel element thus creating resonance phenomena. Based on a simple calculation and experience in the fields, no serious fluctuations in the horizontal force are expected.

If a fluctuation of 10% of the cable forces encountered is assumed, the amplitudes of the movement fluctuations in the longitudinal and transverse directions of the element in phase VII would amount to a maximum of 1 cm with a flow of 2,000 m^3/s. As immersion will take place at a lower discharge rate, the horizontal movement fluctuations in the final phase of immersion will probably be negligibly small.

During immersion (phases VI—VII) the tunnel elements are suspended by cables from four pontoons. In these phases the vertical reaction forces must be absorbed by the pontoons (adequate floating capacity) and by the vertical cables (adequate strength). The vertical forces resulting from the current pressure (all four measured in the model) do not in principle comply with equation (21) given in section 3.3.4 because they are directly influenced by the current and indirectly by rotation of the tunnel element.
This rotation changes the flow pressure at the top and bottom while displacement also occurs of the centre of gravity of the water in the ballast tanks inside the element (see fig. 6). There is a direct relationship between the force in a vertical cable and the vertical displacement of the fixing point on the element (pontoon immersion depth). This relationship is:

$$Kv \approx -V \tag{23}$$

in which
Kv = current force in vertical cable (tf),
V = vertical displacement of cable fixing point (cm).

On the basis of this relationship, it is apparent that the immersion phase VIa—VIb will be decisive for the forces in the vertical cables and that these forces may increase substantially when the flow rates are high (see fig. 24).

As a result of the water flow, a reduction in water level will occur at the tunnel element and a moment with a horizontal axis and a vertical force will act on the element. This moment and force are compensated by reaction forces primarily due to changes in the upward force resulting from vertical displacement and rotation of the tunnel element. Vertical movements of the model are determined by measuring these displacements of three suspension points and calculating from this the displacement of the fourth suspension point. Vertical displacements are highest at tunnel element 3; figure 24 shows the decisive vertical displacement values. This figure clearly shows that the tunnel element loses stability when it is immersed by letting in water ballast and suspending it from the pontoons. From the time at which the element is entirely under water, the vertical reaction forces must be supplied by the pontoons with a much smaller base surface than the element so that greater vertical displacements are needed to obtain the same reaction forces.
Maximum vertical displacements will occur in the immersion phase VIa—VIb.

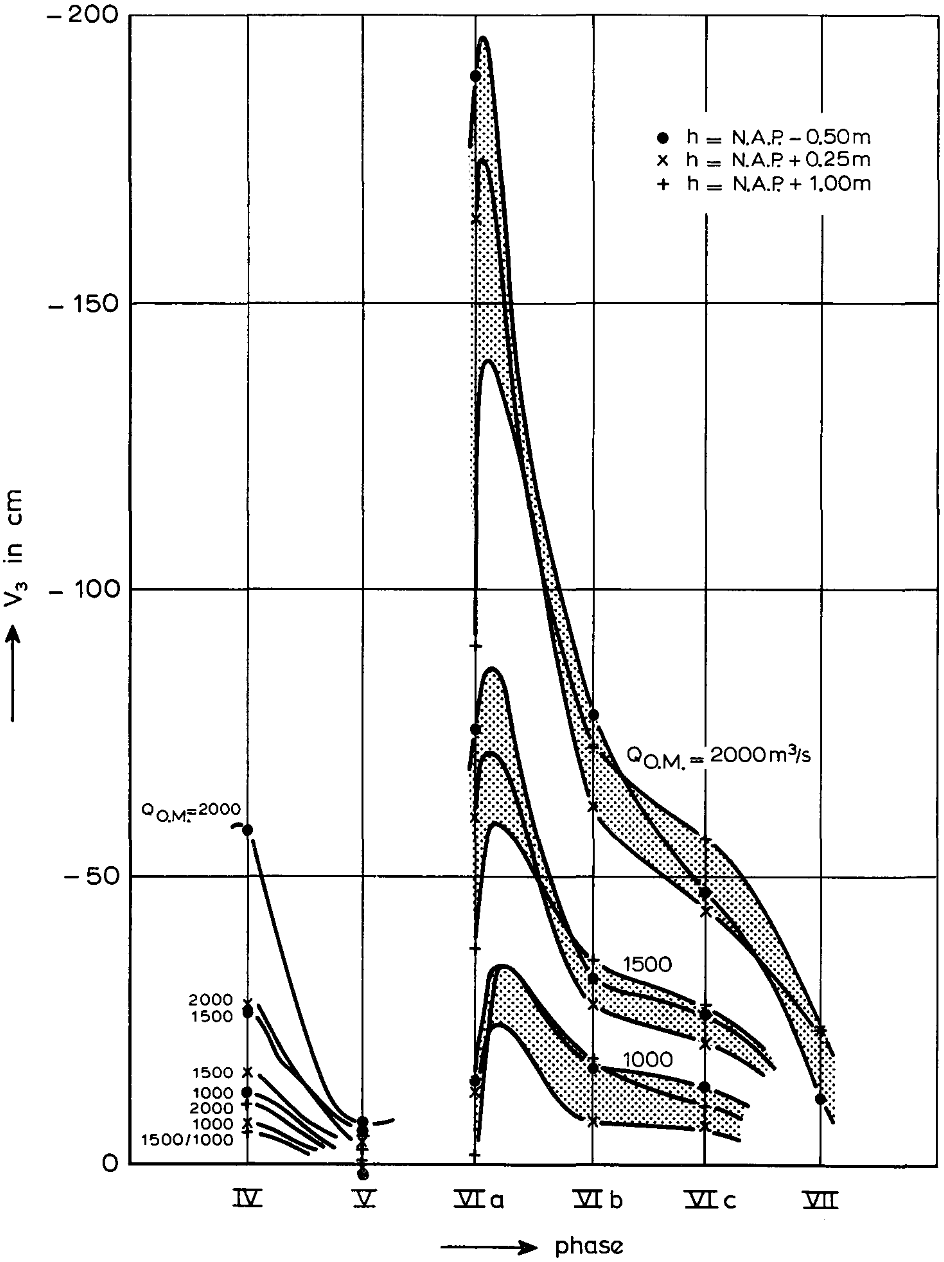

Note: in phases VI and VII $K_{V3} \approx -V_3$
with K_V in tonnes and V in cm

Figure 24. Maximum vertical displacements during positioning of elements 1 and 3.

In this phase there is, however, a sufficient water depth below the element to allow these displacements to occur without risk. A critical moment occurs for tunnel element 3 in phase V—VI when it is drawn past the elements 1 and 2 which have already been immersed. During this phase, the ends of element 3 must pass the ends of elements 1 and 2; at high tide the clearance is barely 1 m. The vertical displacements for element 3 in this critical phase must be between those for phase IV and phase V. The settling values measured for phase IV are probably too high because in this phase the forces on the element are high (see fig. 23) while the settling in phase V will be minimal as a result of the upward current pressure due to the presence of the immersion trench embankment below the element. Measurements show that the downstream side sinks more in phase V than the upstream side. It may be assumed that even under unfavourable conditions ($Q_{O.M.} = 2{,}000$ m^3/s and h = N.A.P. — 0.50 m) settling in the critical phase will be no more than 0.25 to 0.5 m. These considerations mean that even this difficult manoeuvre can be carried out with a satisfactory margin.

3.3.6 *Conclusions*

Based on the results of the model studies in which a wide range of flow conditions were considered, an accurate choice can be made of the equipment to be used (tow power, strength of cables and anchorages for sinking) and the permissible flow conditions.
Based on the choice of equipment and model results for the transport of the elements, a reliable navigation plan can also be drawn up. Programmes can be compiled for immersing the elements in which no risks will be taken in the critical phases (horizontal force in phase IV—V; vertical force in phase IVa—IVb; vertical displacement of tunnel element 3 in phase V—VI).
The cost of the hydraulic study was about 0.5% of the cost of building the Drecht tunnel.

3.4 Tension piles below open approaches

3.4.1 *Introduction*

As indicated in section 3.1, open tunnel approaches are generally built as reinforced concrete through structures consisting of a base slab on which the carriageway is provided and two side walls which must act as a barrier to the horizontal soil and ground water pressures. The base slab and walls on either side form a monolithic structure.
During construction, the base slab will only exert downward forces (dead weight) on the subsoil. After completion of the concrete structure, the excavation is filled up on the outside of the civil engineering structure and drainage is stopped. The

Photo 8. The 'Utrechtse Baan' at The Hague under construction. ▶

ground water which now rises will exert an upward force on the concrete structure which is generally considerably greater than the dead weight of the structure. Although gravity structures have been built (Coen tunnel) it is generally less expensive to deflect the resulting upward forces into the subsoil by means of tension piles which are anchored on the base slabs and introduced into the soil before construction of the base slab begins. For economic reasons preference is generally given to post-tensioned piles made in situe (e.g. of the VIBRO type) rather than precast, prestressed concrete piles.

As the pile foundations are an important cost item in the tunnel approaches (and in the case of other similar structures), at the request of the Locks and Weirs Department of the Rijkswaterstaat, the Delft Soil Mechanics Laboratory carried out a number of prototype tests with a view to limiting the number of piles and their length as far as possible.

Sections 3.4.2 and 3.4.3 describe pulling tests on individual Vibro piles for the Heinenoord tunnel and an underpass with open approaches at Zeist. Section 3.4.4 summarizes tests on groups of piles for the Utrechtse Baan at the Hague (not a tunnel but a 1,700 m long lowered urban motorway in a trough structure, locally crossed by viaducts at street level; see photo 8). In view of the requirement that a horizontal clay layer present in the soil (separating layer between two water-carrying strata with different pressure heads) must remain 'waterproof' even after sinking the piles

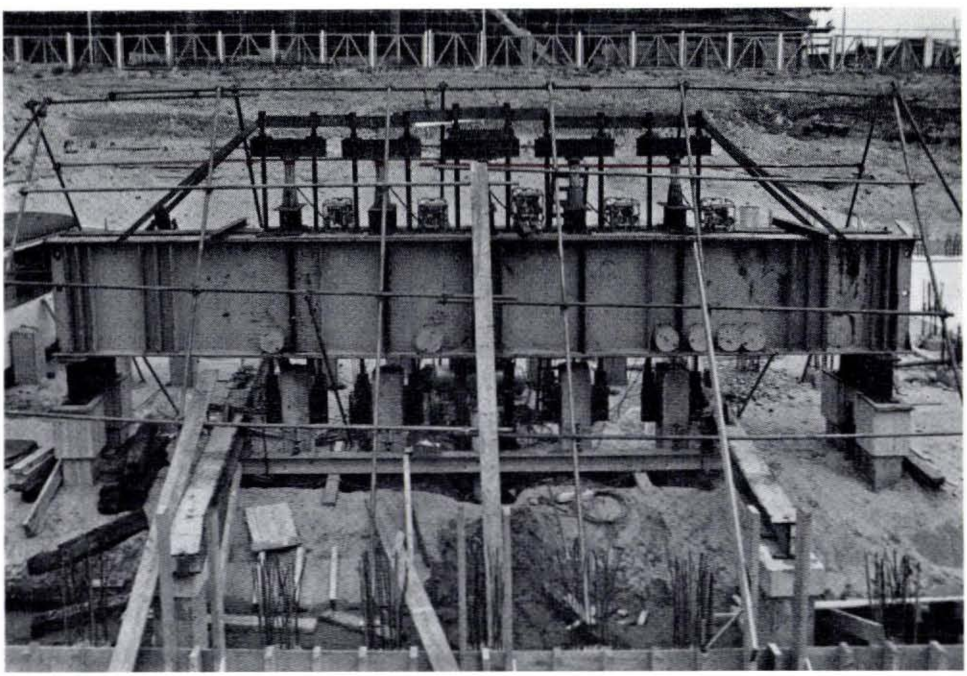

Photo 9. Installation for load test on a pile row at the Utrechtse Baan.

which pass through the clay layer at many points, preference was given in this case to precast prestressed concrete piles rather than piles made in situe.

3.4.2 *Pulling tests at the Heinenoord tunnel*

Pulling tests were carried out on 8 VIBRO piles towards the end of 1967 at the Heinenoord tunnel.
For these 20 m long test piles, 3 different pile base shapes were used, i.e. flat, truncated and pointed (fig. 25). The pile base diameter was 517 mm; the external diameter of the pile-driving tube was 457 mm [lit. 19].

PURPOSE OF THE STUDY

Based on the results of studies with the adhesion jacket cone, data were derived from pulling tests relevant to the method of calculation for this type of pile.
We then determined the influence of the pile base shape on the level of the pulling force.

SOIL STUDY

On the test site a large number of soundings were made both before and after pile construction, with the 'mechanical adhesion jacket cone' and the 'electrical cone friction recorder'.
Figure 26 shows the ground structure which consists of:
— 8 to 9 m of clay and peat locally mixed with a little sand;
— approx. 7 m of sand and sand containing silt in which the sharp reduction in cone resistance is caused by small layers of clay or peat;
— 9 to 10 m of sand which in places contains a little gravel.

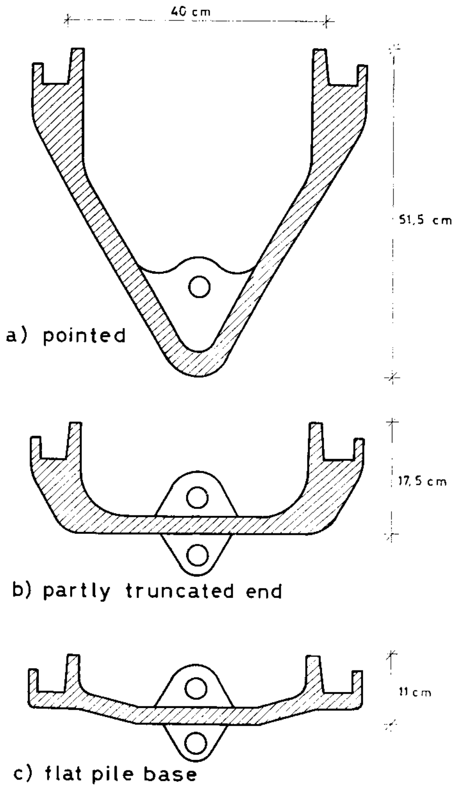

Figure 25. Pile base shapes Heinenoord.

TEST LOAD RESULTS (fig. 27)

Apart from the differences in the pile base shape referred to above, in two of the eight piles the initial tension was 180 tf instead of 60 tf.
Five piles were tested under a loading pattern in which four hours of constant load were immediately followed by five rapid load changes to zero.

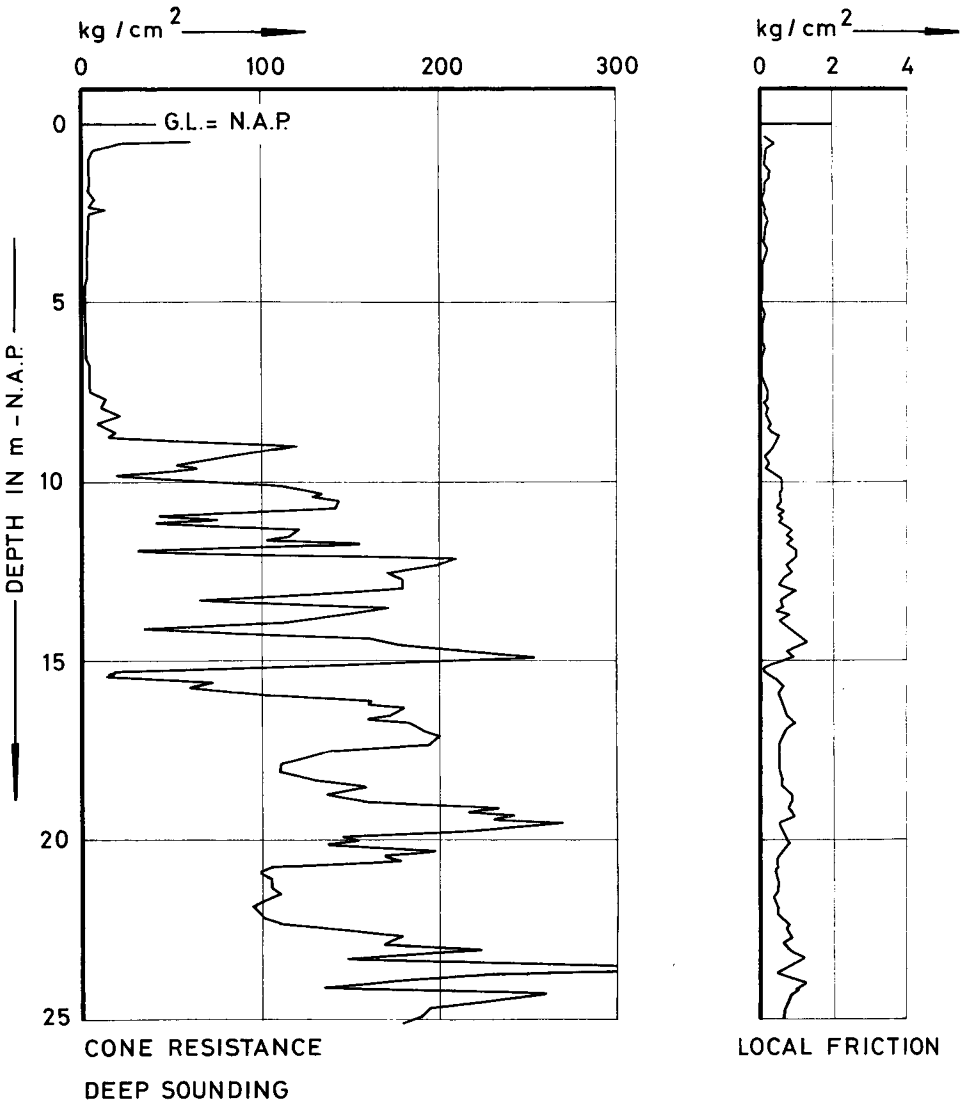

Figure 26. Soil investigation at Heinenoord tunnel.

The other three test piles were loaded according to a pattern in which the different loads were held constant for eight hours. These periods were not followed by rapid load changes.

Finally the two piles with an initial tension of 180 tf were subjected to a fatigue test in which a large number of rapid load changes were also exerted on the piles.

Table 4 shows the result of the different tests.

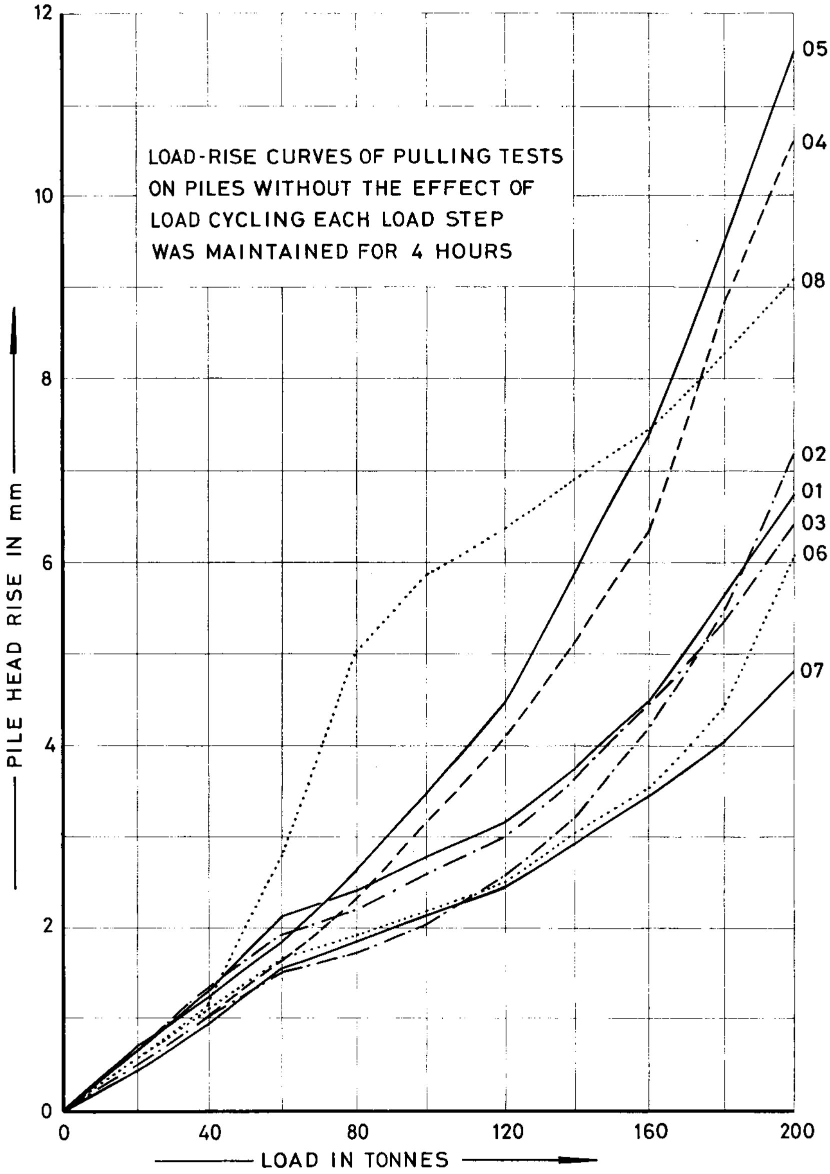

Figure 27. Test load results Heinenoord.

Table 4

	Pile 01	Pile 02	Pile 03	Pile 04	Pile 05	Pile 06	Pile 07	Pile 08
Shape of base	truncated	pointed	flat	flat	pointed	pointed	flat	truncated
Prestressing force (tf)	60	60	60	180	180	60	60	60
Tested with load changes	yes	no	yes	yes	yes	yes	no	no
Permissible pulling force (tf)	150	130	165	180	150	170	185	160
Rise of pile head (mm) at permissible pulling force	4.1	3.3	4.4	8.8	6.5	4.3	5.0	7.8
Ultimate pulling force (tf) based on data from soundings	140	130	147	174	150	195	158	173

The permissible pulling forces indicated in the table were determined by the criterion normally used for this purpose at the Delft Soil Mechanics Laboratory:
i.e. the load which, in the five rapid load changes, causes an additional rise in the pile head of 0.2 mm.
It was possible to use this criterion for all the piles exposed to alternating load.
Where no alternating loads were applied, the permissible load-bearing capacity was determined as one half of the estimated maximum load bearing capacity.
For an accurate comparison of the pulling test results with the ultimate pulling forces calculated from the sounding data, these force values had to be corrected.
This was done with reference to:
— the higher specific weight of the concrete used;
— the reduction in the hydrostatic water pressure of 5.5 to 6 m as a result of the use of drainage pumps;
— the additional height of the concrete in the piles during pile driving.

After correction, the results were found to be approximately 1.6 times higher than was to be expected on the basis of the calculation.
This means in fact that a correction factor of 1.6 should be introduced for long VIBRO piles in the method of calculation described in Lit. 20 and 21.
However, as the tests at Zeist showed, great caution is necessary.
It will aslo be clear that the results of the tests are only valid in the case of piles which do not interact on each other and which are built to the highest standards. The results suggest that the pulling force is not influenced by the shape of the base.
The rise of the pile head is, however, influenced by the magnitude of the prestressing

force and the method by which the tests are carried out, i.e. with or without rapid load changes.
So far no reference has been made to the results of the fatigue tests.
Table 5 gives a summary of these test results.

Table 5

	Pile 04	Pile 05
Permissible pulling force (tf)	180	150
Duration of load	66 hrs 180 tf	57 hrs 180 tf
Rise in pile head (mm) during constant load	0.60	0.68
Rise in pile head (mm) during last 10 hours of constant load	zero	0.1
Number of rapid load changes	29(0 − 180 tf)	30(0 − 145 tf)
Rise in pile head (mm) during load changes	0.70	0.46
Rise in pile head (mm) during last 10 load changes	approx. 0.2	approx. 0.1

During a static fatigue test at the permissible pulling force, the rise in the pile head does in fact approach a limit. The piles come to rest.
As a consequence of the load changes, the piles do not come to rest. As is known in the case of piles exposed to a practically constant pulling force, a safety coefficient of 2 is used. Clearly with extremely high load changes, a higher safety coefficient would be desirable.

3.4.3 *Pulling tests at the Zeist underpass*

On a test site at Zeist, 6 short VIBRO piles (7, 8 and 9 m) were subjected to pulling tests. The piles were driven with a 457 mm Ø pile driving tube and a flat pile base, Ø 517 mm [lit. 22].

PURPOSE OF THE STUDY

Is the correlation with sounding data found at Heinenoord also applicable to short VIBRO piles?
Is there any relaxation of tension?
What is the influence of a lowered ground water level on the size of the permissible pulling force?

Soil study

To determine the soil characteristics at the location of the test piles, seven soundings were taken with the mechanical adhesion jacket cone and twelve soundings with a constricted electrical cone friction meter (construction length 435 mm).
These tests showed that down to about 12 m below the surface the subsoil consisted primarily of a moderately firm sand structure with cone resistances between 40 and 120 kg/cm^3 and local firmer layers. In one of the tests the cone resistances at a depth of 3.5—8 m below the surface were found to be only about 20 kgf/cm^2. Figure 28 shows the soil characteristics.

Test load results (fig. 29)

In all the pulling tests, the load pattern used consisted of 4 hours constant load followed by 4 rapid load repetitions.
Two of the piles were tested again after about one year. The ground water level was still lowered in the tests.
On two other piles, the pulling test was repeated after about $1\frac{1}{2}$ years. The ground water level was then at its original level.
The pulling test results and a comparison of the pulling forces calculated from the sounding data are shown in table 6.
It is striking that the influence of the pile length on the pulling capacity of the piles is only slight.
This must be related to the characteristics of the soil or to changes in the latter due to the construction of the piles.
Subsequent soundings 013 to 018 (see fig. 30) show that the cone resistance down to a depth of about 7 m below the surface is considerably higher than in the sand stratum situated underneath.
The same tendency was also observed for local friction. A substantial part of the pulling force is in fact derived from friction over the lowest section of the pile while friction in the central part of the pile is considerably reduced. In the type of soil described here, this means that a pile with a length exceeding 7 m cannot derive much more strength from the soil.
This is reflected in the calculated maximum pulling forces shown in line 8 of table 6.
Figure 29 shows the load rise diagrams for all the tension tests.
It is apparent that the behaviour of the piles in the 2nd and 3rd series of tests up to the originally determined permissible load capacity is much the same as that of the similar pile in the first series of tests. Above this load the deformation characteristic is noticeably different. Much greater displacements occur and the pulling force limit is reached earlier.
To calculate the maximum pulling capacity, three groups of soundings are available,

Table 6

1	pile number	02	011	04	05	03	08
2	pile length (m)	9	9	8	8	7	7
3	max pulling force (tf) (first series of pulling tests)	160 to 165	180	165	180	165	135
4	load (tf) at 0.2 mm extra rise (first series of pulling tests)	75	80	80	92.5	82.5	62.5
5	maximum pulling force (tf) (2nd and 3rd series of pulling tests)	105	105	105	–	90	–
6	load (tf) at 0.2 mm extra rise (2nd and 3rd series of pulling tests)	75	72.5	80	–	65	–
7	Max. pulling force (tf) according to preliminary sounding	95	106	83	99	68	69
8	Max. pulling force (tf) according to soundings after 1st series of pulling tests	122	120	114	122	121	87
9	Max. pulling force (tf) according to soundings after 2nd & 3rd series of pulling tests	110	90	104	–	74	—
10	Relationship of test load results in 1st series to first forecast	1.68 to 1.74	1.70	1.99	1.82	2.42	1.94
11	Relationship of test load results in 1st series to calculated results for 2nd group of soundings (013-018)	1.31 to 1.35	1.50	1.45	1.48	1.36	1.54
12	Relationship of test load results in 2nd & 3rd series to calculated results for 3rd group of soundings (019-022)	0.95	1.17	1.01	–	1.21	–
13	Relationship of test load results in 2nd & 3rd series to calculated results of initial soundings	1.10	0.99	1.26	–	1.32	–

i.e. prior to pile construction, after pile construction (and the first test) and after the third series of tests (fig. 30). The calculation result obtained by introducing a correlation factor of 1 in the current method of calculation is shown in lines 7, 8 and 9 of table 6 for the different soundings.
The results show that substantially higher maximum pulling forces can be expected as a consequence of pile construction (see lines 7 and 8).
The average increase is 25%. After about $1\frac{1}{2}$ years, the increase only seems to be some 10%. Clearly, relaxation has occurred.
The test load results in fact show the same tendency. To begin with the result was

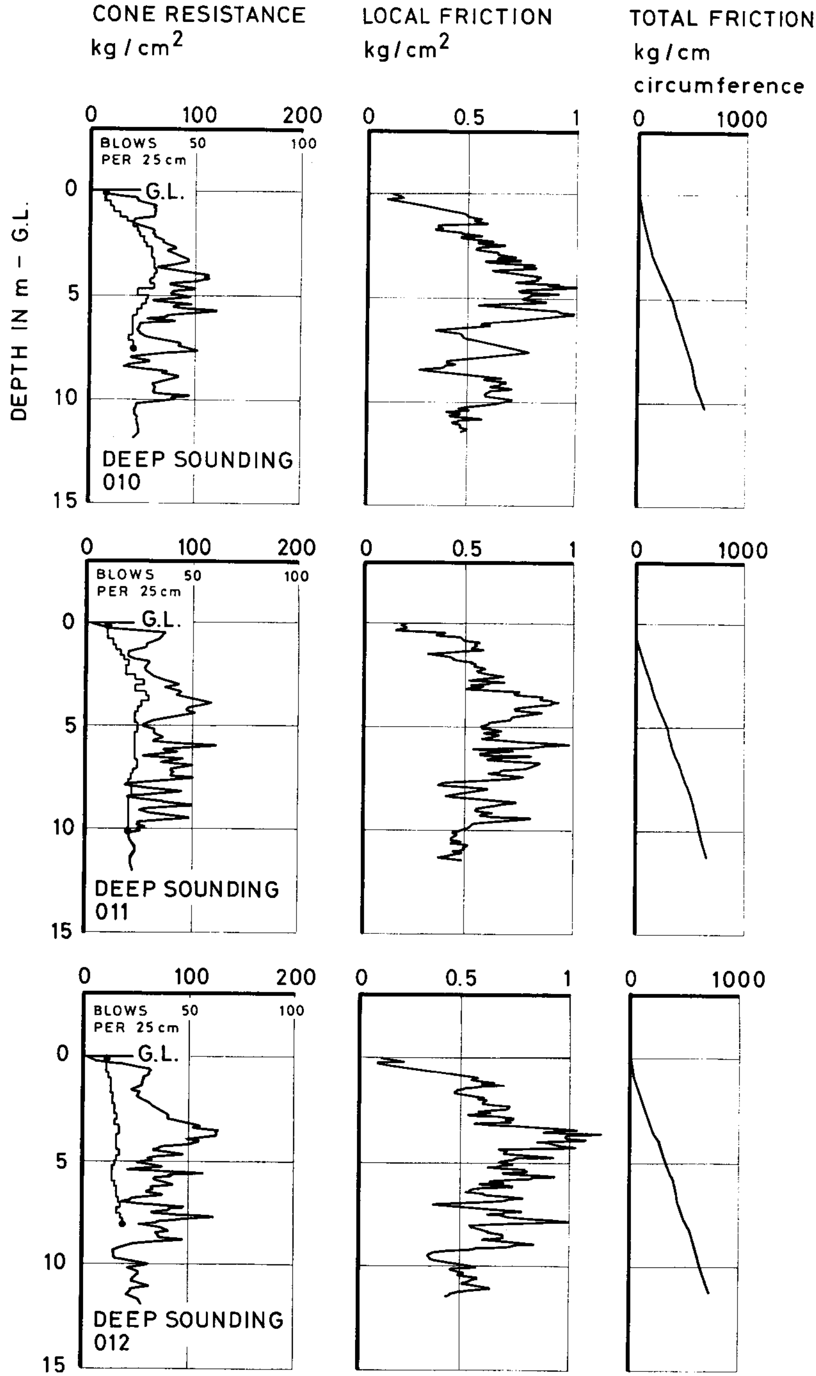

Figure 28. Soil investigation at Zeist underpass.

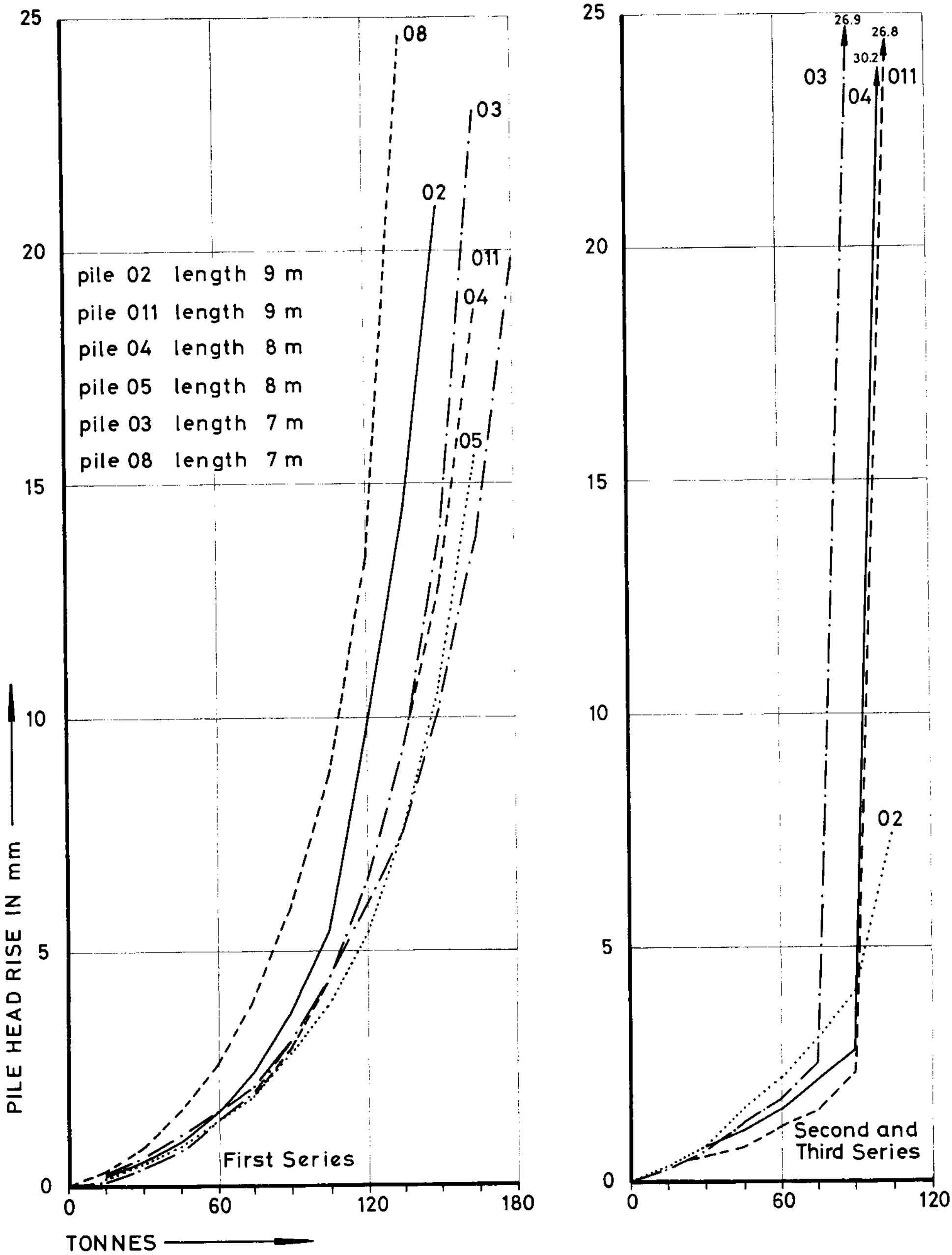

Figure 29. Test load results Zeist.

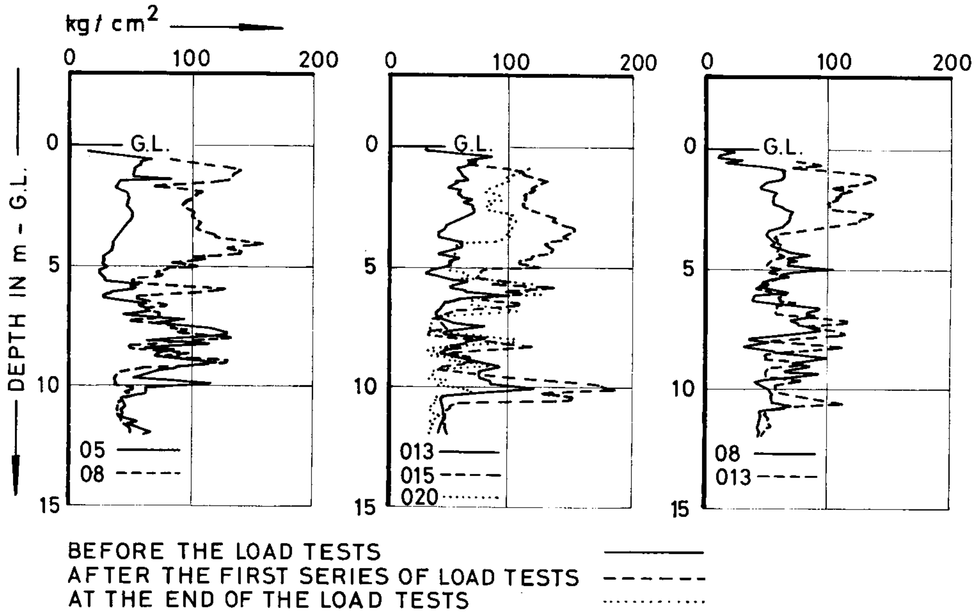

Figure 30. Soundings at Zeist.

on average some 85% better than expected (Table 6, line 10). However, if the first series of test load results is compared with the 2nd group of soundings (line 11), the pulling test results are found to be only about 45% better. On comparison of the 2nd and 3rd series of test loads with the last group of soundings an average improvement of about 10% still remains.

If the results are also compared with the calculation results from the 1st group of soundings, a mean improvement of about 15% is found.

In the worst instance represented by the last two comparisons, there is no improvement at all.

As a result of the evident relaxation, the correlation coefficient probably does not exceed the minimum calculated value of 1.

Because of the observed relaxation, a correlation coefficient of 1 would no doubt be more appropriate for long piles than the value ascertained in the pulling tests at Heinenoord. It is unfortunately impossible to draw any clear conclusion on the influence of a lowering of the ground water level on the maximum load capacity of short VIBRO piles. There seems to be some influence but because the ground water level differences in these tests were very low, it cannot be quantified.

The influence on the maximum pulling force may be quantifiable if the ground water level differences are substantial.

The reader will of course be aware that the correlation factor referred to can only hold good when there is no mutual interaction between the piles.

If such interaction exists, the calculated pulling force must be reduced. The pulling tests at the Hague discussed below considered this aspect in more detail.

3.4.4 *Pulling tests at the Utrechtse Baan in the Hague*

In mid-1972, a study was made at the through structure of the Utrechtsebaan of the pulling load capacity of precast, prestressed concrete piles. These piles, 380 mm square, had a flat or pointed pile base. The base level of the piles was fixed at 17.50 m —N.A.P. while the level of the construction cutting base was 6.00 m—N.A.P.

Purpose of the study

To determine and compare the pulling capacity of piles with a flat base and piles with a pointed base. Determination of the 'group effect'.

Test structure and soil study

One pile with a flat base and one pile with a pointed base were driven on the test site. In addition, a series of five piles with a pointed base and five piles with a flat base were also driven.

The distance between the piles in the series was 1.10 m. All the piles were subjected to a test load following the usual pattern, constant loading being followed by load changes to zero.

For the tests of the individual piles, stress control was used; for the two series of piles, strain control was used because of the fact that piles below a rigid tunnel base should all deform in the same way while the forces on each pile may differ.

The site investigation included four soundings from the original ground level (approx. 0.60 m + N.A.P.), four soundings from the bottom of the excavation before pile driving and six soundings after pile driving.

Figure 31 shows the soil characteristics at the pile location both before and after excavation.

From the original ground level down to approx. 1.00 m - N.A.P. soil is found with a very heterogeneous composition and extremely low cone resistances. Below this layer down to about 4.00 m - N.A.P. there is a layer of clay and peat with low cone resistances.

From 4.00 m down to approx. 9.00 m - N.A.P. the principal material encountered is sand with widely varying cone resistances.

This layer was interspersed with clay and peat impurities which caused sharp reductions in cone resistance. In the layer from 9.00 m to 13.00 m - N.A.P. the soil consists of a fairly homogeneous sand stratum with cone resistances of about 100 kgf/cm^2. Below this layer there is a clay stratum with a thickness of about 4 m (cone resistances = 10 kgf/cm^2), followed at 17.00 m - N.A.P. by a sand layer in which the cone resistances rapidly rise to 150 kgf/cm^2 or even higher values.

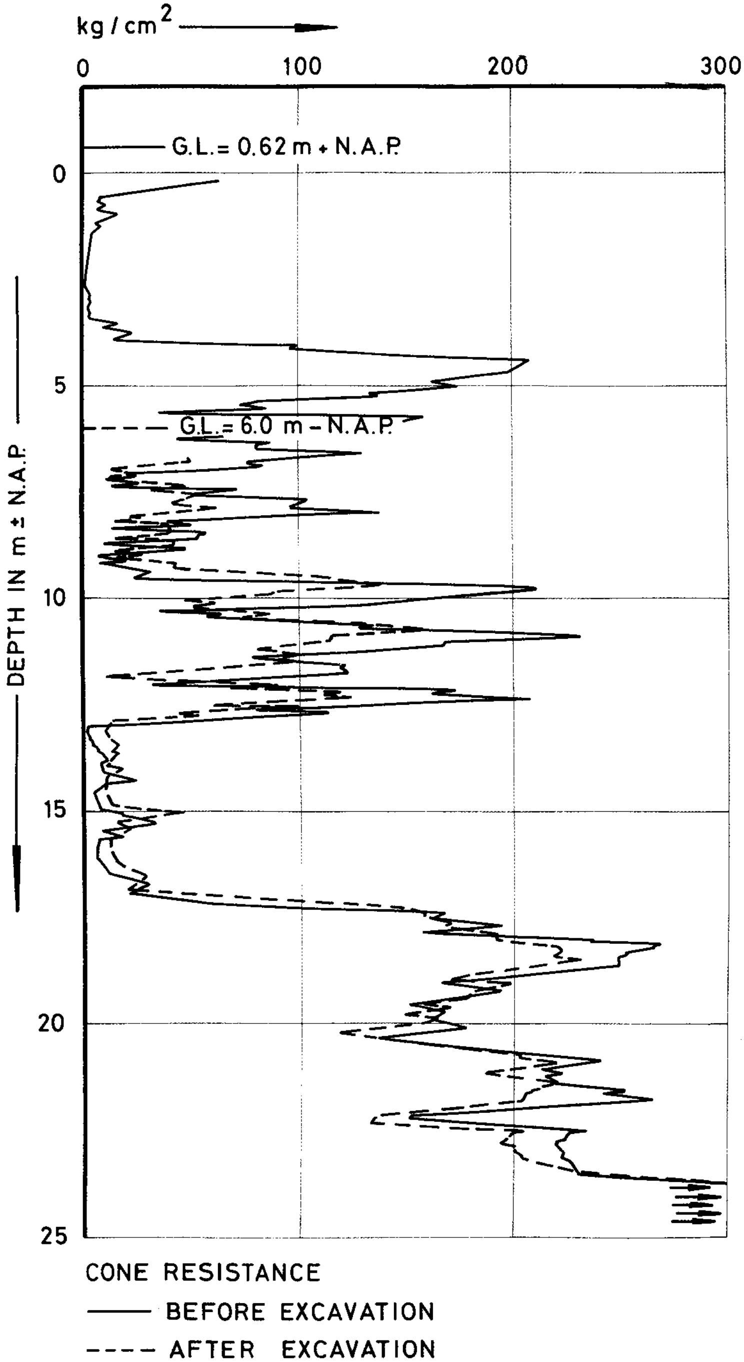

Figure 31. Soil investigation at Utrechtse Baan.

Comparison of the sounding results indicated a low reduction in the measured cone resistances as a result of excavation. After driving the piles, a sounding pattern corresponding approx. to the original values was found again. Clearly, the low reduction in cone resistance caused by the excavation was completely compensated by the compression due to pile driving. The maximum pulling forces for the piles were calculated on the basis of the sounding data.

TEST LOAD RESULTS

During the tests of the pile with the pointed base, the maximum pulling force was found to be somewhat higher than the capacity which the tension installation could handle. The maximum pulling force was therefore estimated at between 110 and 115 tf on the basis of the pattern of deformation. In the light of the measured rise in the pile head under constant loading and the additional rise in the pile head which occurred during rapid load changes to zero, the permissible pulling force was fixed in the first instance as approx. 75 tf.
This value is, however, too high for safety. The permissible pulling force is therefore taken as equal to half the maximum pulling force, i.e. 55 tf.
On exposure to this load, the pile head rose by about 1.8 mm. The pulling test on the individual pile with the flat base gave a maximum pulling force of 100 to 105 tf. This gives a permissible pulling force of just over 50 tf (safety coefficient 2). On exposure to this load, the pile head rose by approx. 1.6 mm. In this case too, a higher permissible pulling force may be fixed, i.e. approx. 72 tf, because of the deformation characteristic of the pile under constant loading and load changes.
The tests on the series of piles were conducted with a maximum capacity of 60 tf per pile.
Since the piles developed an unexpectedly high pulling force, the maximum pulling force is not reached for any pile in the series.

Consequently this maximum load had to be estimated from the deformation characteristic and comparison with the deformation characteristic of the individual piles. Table 7 shows all the maximum pulling forces.

The maximum pulling forces were calculated from the sounding data by the method already described for this purpose. A correlation factor of 1 was again taken as the basis for this calculation. Comparison of the pulling test results with the calculated maximum pulling forces indicates the correlation factor which should be used in practice. These values are shown in Table 8 and also indicated in Figure 32.

These results show that:
The correlation factors (pile factors) of the two individual piles differ only slightly and correspond to a value of about 1.

Table 7

	Max. pulling force (tf) Piles with pointed base	Max. pulling force (tf) Piles with flat base
Individual pile	110 to 115	100 to 105
Edge pile 1	approx. 90	approx. 81
Central pile 2	,, 85	,, 65
Central pile 3	,, 77	,, 52
Central pile 4	,, 76	,, 71
Edge pile 5	,, 91	,, 81
Average	,, 84	,, 71
Edge piles average	,, 90	,, 81
Central piles average	,, 79	,, 63

Table 8

	Pile factors Piles with pointed base	Pile factors Piles with flat base
Individual piles	approx. 1.12	approx. 1.02
Edge pile 1	,, 0.89	,, 0.80
Centre pile 2	,, 0.84	,, 0.64
Centre pile 3	,, 0.76	,, 0.51
Centre pile 4	,, 0.74	,, 0.70
Edge pile 5	,, 0.90	,, 0.80
Average	,, 0.83	,, 0.70
Edge piles average	,, 0.89	,, 0.80
Centre piles average	,, 0.78	,, 0.62

The correlation factors for the pointed base pile are in each case slightly higher (approx. 10%) than for the flat base pile.
The correlation factors for the individual piles are noticeably higher than for any pile in the series.
The correlation factors for the edge piles are substantially higher than for the centre piles.
Clearly, the piles in two series influence each other. The piles are situated within the area of mutual interaction.

The deformation characteristic shows that with a load corresponding to 50% of the maximum pulling force ($n = 2$) the pile head rises in all cases by about 1.5 to 2 mm.

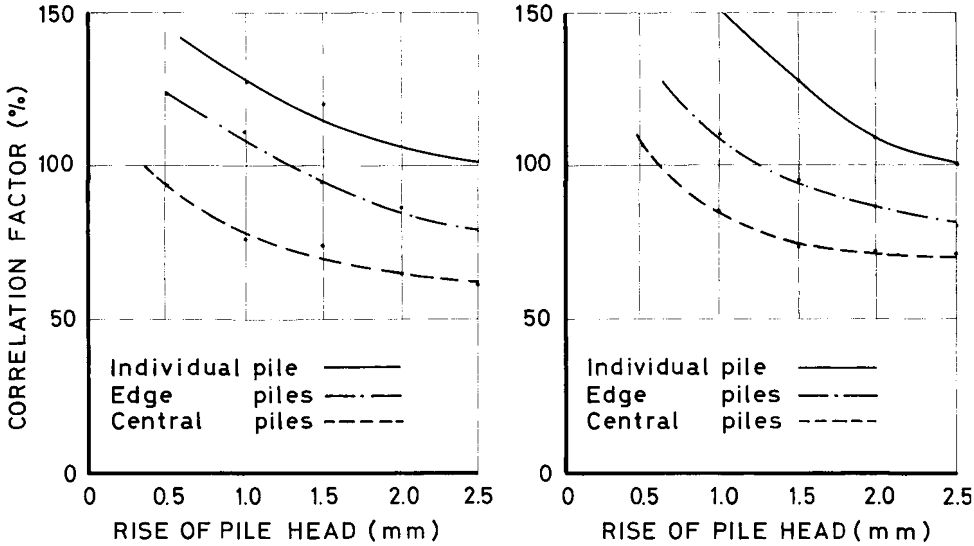

Figure 32. Utrechtse Baan; comparison of correlation factor with pile head rise (left: piles with flat base; right: piles with pointed base).

3.4.5 *Conclusion*

It should be noted in conclusion that the pulling tests discussed above have considerably increased our knowledge of the behaviour of tension piles. Nevertheless, in each individual case, the input data for the method of calculation to be used must be assessed very critically. Apparently slight differences in the soil characteristic regularly cause substantial differences in the load-bearing capacity of piles. It is therefore vital to increase our knowledge, among other things by carrying out load tests.

Literature

A Descriptions of road tunnels in the Netherlands

[1] Maas tunnel: ir. J. P. van Bruggen in 'De Ingenieur' 1939, No. 41; M. Lassen Nielsen in 'De Ingenieur' 1941, No. 27.

[2] Velsen tunnel: ir. A. Eggink in 'De Ingenieur' 1953, No. 36, 1954, No. 40, 1956, No. 4; ir. G. Vooys in 'De Ingenieur' 1954, No. 40.

[3] Coen tunnel: ir. A. Eggink, ir. H. C. Wentink, ir. A. Griffioen and Ch. J. de Vilder respectively in the following numbers of the 1963 volume of 'De Ingenieur': 35, 37, 39 and 41.

[4] Benelux tunnel: ir. H. Engel and ing. J. C. van Dusschoten in 'Land en Water' 1967, No. 2 (English edition).

[5] Heinenoord tunnel: ir. H. C. Wentink in 'Land en Water' 1967, No. 2 (English edition).

[6] IJ tunnel: ir. B. Jansen in 'De Ingenieur' 1964, Nos. 9, 11 & 14; ir. A. T. J. van Veen in 'De Ingenieur' 1964, No. 25; ir. L. P. Sikkel in 'De Ingenieur' 1965, Nos. 13, 15 & 17.

[7] Vlake tunnel: ir. B. P. Rigter in 'Land en Water' 1974, No. 5.

B Description of other tunnels in the Netherlands built by the immersed tube method

[8] Subway tunnel in Rotterdam: ir. G. Plantema in 'Civil Engineering — ASCE', August 1965.

[9] Underground conduit at Jutphaas and pipeline tunnels under the Hollandsch Diep and Oude Maas: ir. A. Glerum in 'Tunnels and Tunnelling', July-August 1973.

C Other subjects

[10] 'Ontwerp-richtlijnen voor het ontwerp van wegen', Rijkswaterstaat, Dienst Verkeerskunde (in particular: Chapter III: 'Dwarsprofielen'').

[11] Report 1971 of the Technical Committee on Road Tunnels of the Permanent International Association of Road Congresses (PIARC, Paris).

[12] Ir. A. Griffioen and R. v. d. Veen: 'Foundation of a tunnel by the sand flow system' in 'Tunnels and Tunnelling', July-August, 1973.

[13] 'Rapport over een vergelijkend onderzoek naar de invloed van enige cementsoorten op enkele eigenschappen, die verband houden met scheurvorming in beton' in 'Cement' 1963, No. 1.

[14] Dr. ir. Walter Schleeh: 'Die Zwängspannungen in einseitig festgehalten Wandscheiben' in 'Beton- und Stahlbetonbau' 3/1962.

[15] Toshikazu Kawamoto: 'Fundamental photo-elastic studies on shrinkage stresses in massive structures', Proc. of the 8th Japan National Congress for Appl. Mechanics, 1958, page 225.

[16] R. E. Copeland: 'Shrinkage and temperature stresses in masonry', Journal of the A.C.I., Feb. 1957, page 769.

[17] Dr. Ing. Wolfgang Mandry: 'Über das Kühlen von Beton', Springer Verlag, 1961.

[18] B. Verkerk en H. van der Zanden: 'Betontechnologische aspecten bij de Metrobouw' in 'Cement' 1973, No. 8.

[19] Ir. L. W. A. van den Elzen: 'Trekproeven op in de grond gevormde palen met variërende paalvoetvorm, Heinenoordtunnel', L.G.M.-mededelingen DL XIII, No. 3.

[20] Dr. ir. H. K. S. Ph. Begemann: 'The maximum pulling force on a single tension pile calculated on the basis of results of deep soundings with the adhesion jacket cone', Proceedings of the 6th International Conference on Soil Mechanics and Foundation Engineering, Canada 1965 (Volume 2).

[21] Dr. ir. H. K. S. Ph. Begemann: 'The Dutch static penetration test with the adhesion jacket cone', L.G.M.-mededelingen DL XIII, No. 1.

[22] W. F. Heins: 'Trekproeven op, volgens het VIBRO-systeem in de grond gevormde palen van geringe lengte te Zeist', L. G. M.-mededelingen DL XV, No. 3.

D Articles published since this communication was written

[23] Report 1975 of the Technical Committee on Road Tunnels of the Permanent International Association of Road Congresses (PIARC, Paris).

[24] Drecht tunnel: ir. H. J. C. Oud, ir. J. v. Geest and ir. V. L. Molenaar in 'Cement' 1974, No. 12.

[25] Kil tunnel: ir. C. A. Beerepoot, ir. G. J. v. Herrewegen and ir. H. J. C. Oud in 'Wegen' 1975, No. 5.

[26] Margriet tunnel: ir. P. Kieft, P. J. M. v. Kinderen and J. H. Resink in 'Cement' 1976, No. 4.

Photographs:

Slagboom and Peters: No. 1.

Rijkswaterstaat: No's. 2, 3, 5, 6.

Verschoore: No. 4.

Delft Hydraulics Laboratory: No. 7.

Dick Lemcke: No. 8.

Soil Mechanics Laboratory: No. 9.

In the series of Rijkswaterstaat Communications the following numbers have been published before:

No. 1.* *Tidal Computations in Shallow Water*
Dr. J. J. Dronkers† and prof. dr. ir. J. C. Schönfeld
Report on Hydrostatic Levelling across the Westerschelde
Ir. A. Waalewijn, 1959

No. 2.* *Computation of the Decca Pattern for the Netherlands Delta Works*
Ir. H. Ph. van der Schaaf† and P. Vetterli, Ing. Dipl. E.T.H., 1960

No. 3.* *The Aging of Asphaltic Bitumen*
Ir. A. J. P. van der Burgh, J. P. Bouwman and G. M. A. Steffelaar, 1962

No. 4. *Mud Distribution and Land Reclamation in the Eastern Wadden Shallows*
Dr. L. F. Kamps†, 1962

No. 5. *Modern Construction of Wing-Gates*
Ir. J. C. le Nobel, 1964

No. 6. *A Structure Plan for the Southern IJsselmeerpolders*
Board of the Zuyder Zee Works, 1964

No. 7. *The Use of Explosives for Clearing Ice*
Ir. J. van der Kley, 1965

No. 8.* *The Design and Construction of the Van Brienenoord Bridge across the River Nieuwe Maas*
Ir. W. J. van der Eb†, 1968

No. 9. *Electronic Computation of Water Levels in Rivers during High Discharges*
Section River Studies. Directie Bovenrivieren of Rijkswaterstaat, 1969

No. 10.* *The Canalization of the Lower Rhine*
Ir. A. C. de Gaay and ir. P. Blokland†, 1970

No. 11.* *The Haringvliet Sluices*
Ir. H. A. Ferguson, ir. P. Blokland† and ir. drs. H. Kuiper, 1970

No. 12. *The Application of Piecewise Polynomials to Problems of Curve and Surface Approximation*
Dr. Kurt Kubik, 1971

No. 13. *Systems for Automatic Computation and Plotting of Position Fixing Patterns*
Ir. H. Ph. van der Schaaf†, 1972

No. 14. *The Realization and Function of the Northern Basin of the Delta Project*
Deltadienst of Rijkswaterstaat, 1973

No. 15. *Fysical-Engineering Model of Reinforced Concrete Frames in Compression*
Ir. J. Blaauwendraad, 1973

No. 16. *Navigation Locks for Push Tows*
Ir. C. Kooman, 1973

No. 17. *Pneumatic Barriers to reduce Salt Intrusion through Locks*
Dr. ir. G. Abraham, ir. P. van der Burg and ir. P. de Vos, 1973

No. 18. *Experiences with Mathematical Models used for Water Quality and Water Quantity Problems*
Ir. J. Voogt and dr. ir. C. B. Vreugdenhil, 1974

In the series of Rijkswaterstaat Communications the following numbers have been published before (continuation):

No. 19. *Sand Stabilization and Dune Building*
Dr. M. J. Adriani and dr. J. H. J. Terwindt, 1974

No. 20. *The Road-Picture as a Touchstone for the three dimensional Design of Roads*
Ir. J. F. Springer and ir. K. E. Huizinga (also in German), 1975

No. 21. *Push Tows in Canals*
Ir. J. Koster, 1975

No. 22. *Lock Capacity and Traffic Resistance of Locks*
Ir. C. Kooman and P. A. de Bruijn, 1975

No. 23. *Computer Calculations of a Complex Steel Bridge verified by Model Investigations*
Ir. Th. H. Kayser and ir. J. Binkhorst, 1975

No. 24. *The Kreekrak Locks on the Scheldt-Rhine Connection*
Ir. P. A. Kolkman and ir. J. C. Slagter, 1976

---

*) out of print

ISBN 90 12 01188 4

606201*